



# Particle physics violating crypto-nonlocal realism

## Entangled mesons

Yu Shi<sup>1,a</sup>, Ji-Chong Yang<sup>1,2</sup>

<sup>1</sup> Department of Physics, Fudan University, Shanghai 200433, China

<sup>2</sup> Department of Physics, Liaoning Normal University, Dalian 116029, China

Received: 14 February 2020 / Accepted: 2 September 2020 / Published online: 18 September 2020

© The Author(s) 2020

**Abstract** It has been well established that quantum mechanics (QM) violates Bell inequalities (BI), which are consequences of local realism (LR). Remarkably QM also violates Leggett inequalities (LI), which are consequences of a class of nonlocal realism called crypto-nonlocal realism (CNR). Both LR and CNR assume that measurement outcomes are determined by preexisting objective properties, as well as hidden variables (HV) not considered in QM. We extend CNR and LI to include the case that the measurement settings are not externally fixed, but determined by HV. We derive a new version of LI, which is then shown to be violated by entangled  $B_d$  mesons, if charge–conjugation–parity (CP) symmetry is indirectly violated, as indeed established. The experimental result is quantitatively estimated by using the indirect CP violation parameters, and the maximum of a suitably defined relative violation is about 2.7%. Our work implies that particle physics violates CNR. Our LI can also be tested in other systems such as photon polarizations.

## 1 Introduction

In 1935, Einstein, Podolsky and Rosen (EPR) questioned the completeness of QM, by applying a criterion of LR to a pair of particles in a quantum state which Schrödinger subsequently referred to as entangled [1,2]. Locality means that two events cannot have any mutual physical influence if they are spacelike separated, that is, their spatial separation is larger than the distance the fastest physical signal, i.e. the light, can travel within the time difference between the two events. In 1964, Bell proposed the first BI satisfied by any local realistic theory while violated by QM [3]. A more experimentally suitable version of BI, called Clauser–Horne–Shimony–Holt inequality [4], was demonstrated to be violated in many experiments, including the ones closing

the locality loophole [5,6], the detection loophole [7,8], and both [9–11]. To close yet another loophole called measuring setting or freedom of choice loophole, observations of Milky Way stars [12,13] and human choices [14] have been employed. Great progress has been made in making use of quantum entanglement in quantum information science.

With the conflict between LR and QM well established, it is important to identify which aspects of LR are the sources of the conflict. For this purpose, Leggett in 2003 proposed the LI, which is satisfied by CNR and is violated by QM [15]. This means that even nonlocal realism, at least a subset, cannot avoid the conflict with QM, so the source of conflict seems to be more likely realism. In 2007, a version of LI was experimentally demonstrated to be violated by using polarizations of entangled photons generated in spontaneous parametric down conversion, first under an additional assumption of rotational invariance [16], then without this assumption [17,18]. LI violation was also demonstrated by using polarizations of photons from fibre-based source [19], as well as the orbital angular momenta of photons [20]. Similar phenomena were observed in different degrees of freedom of single particles [21,22]. Various extended discussions have also been made [23–26].

It is highly interesting to extend the investigations on BI and LI to particle physics, of which standard model (SM) is based on quantum field theory combining QM with special relativity, emphasizing causality and using local gauge principle to describe fundamental interactions. Massive and possibly unstable particles governed by strong and weak interactions and flying in relativistic velocities represent a new class beyond both photons and nonrelativistic particles governed merely by electromagnetism, and can still easily achieve spacelike separation. Besides, one might also wonder whether high energy particles, as excitations of quantum fields, may display nonlocal effects.

In particle physics, entanglement, more often called EPR correlation, has been noted in pseudoscalar meson pairs since

<sup>a</sup>e-mail: [yushi@fudan.edu.cn](mailto:yushi@fudan.edu.cn) (corresponding author)

1960s [27–30]. Various discussions were made on its rigorous verification [31, 33–37], which was experimentally done in  $K^0\bar{K}^0$  pairs produced in proton–antiproton annihilation [38], in  $\phi$  resonance [39–41], as well as in  $B_d^0\bar{B}_d^0$  pairs produced in  $\Upsilon(4S)$  resonance [42–44]. Entanglement is routinely used to tag mesons by identifying their entangled partners [41, 44–49]. Moreover, entangled meson pairs are used in measuring various parameters [48–53], and studying violations of discrete symmetries [54–60], including CP [54, 55, 61–66], time reversal (T) [67–71], and CPT [72, 73]. A possible scheme of teleporting mesons was also proposed [74–76]. There exists similar entanglement in hyperon pairs generated from electron–positron annihilation, which was used recently to measure the phase between the amplitudes of the decays to different helicity states [77].

Many proposals had been made on BI test in entangled mesons [78, 80–86], and in the analogous spin-entangled particles [87–92]. There had been an early experiment using entangled protons to test BI under a few additional assumptions [93]. There was an experiment using entangled  $B_d^0\bar{B}_d^0$  pairs to test BI, in which meson decay acts as effective measurement settings [42]. However, it was not regarded as a genuine Bell test, because of the lack of active measurement [44, 87, 94–96]. Basically this is a manifestation of the loophole of measurement settings, for the following reason. One can envisage a local HV (LHV) theory in which HVs in the source of the particle pairs determine the times, modes and even products of the decays, and the information is carried by the particles, consequently the two particles are secretly correlated no matter how far away they are separated, rendering the violation of BI. Other approaches to BI using entangled high energy particles are difficult to realize, as the alternative bases of measurement are physically limited.

In this paper, we extend CNR and LI to include the case that the measurement settings are not externally fixed, but determined by HV, therefore the above situation jeopardizing BI test in entangled mesons is allowed in CNR, and we propose LI test using entangled neutral  $B_d$  mesons. From QM calculation of single particle decays, we identify the time-dependent effective measuring directions due to the decays, as counterparts of the directions of the polarizers measuring the photon polarizations. For different decay times, they all lie on a plane and a cone, respectively. For such effective measuring directions, whether it is externally fixed or emerge from averages of measurement outcomes over HV, we derive a new version of LI, which is violated by QM and entangled  $B_d$  mesons. We calculate the measurable quantities characterizing the relative magnitude of the LI violation, and find their maxima to be about 2.7%. It turns out that the LI can only be violated when CP symmetry is violated indirectly, i.e. in the mass matrix. Our work establish the true randomness of particle decay, including its time, mode, and product.

On the other hand, our new LI can also be tested in other systems such as photon polarizations.

## 2 Pseudoscalar neutral mesons

In QM, a neutral pseudoscalar meson  $M$  can be regarded as living in a two-dimensional Hilbert space, with basis states  $|M^0\rangle$  and  $|\bar{M}^0\rangle$ , which are flavor eigenstates and mutual CP conjugates, i.e.  $CP|M^0\rangle = |\bar{M}^0\rangle$ ,  $CP|\bar{M}^0\rangle = |M^0\rangle$ . In this basis, the mass matrix is

$$H \equiv \mathbf{M} - \frac{i}{2}\Gamma = \begin{pmatrix} H_{00} & H_{0\bar{0}} \\ H_{\bar{0}0} & H_{\bar{0}\bar{0}} \end{pmatrix}, \quad (1)$$

where  $H_{00} \equiv \langle M^0|H|M^0\rangle$ ,  $H_{0\bar{0}} \equiv \langle M^0|H|\bar{M}^0\rangle$ , and so on. The eigenstates of  $H$  are

$$\begin{aligned} |M_1\rangle &= \frac{1}{\sqrt{|p|^2+|q|^2}} [p|M^0\rangle + q|\bar{M}^0\rangle], \\ |M_2\rangle &= \frac{1}{\sqrt{|p|^2+|q|^2}} [p|M^0\rangle - q|\bar{M}^0\rangle], \end{aligned} \quad (2)$$

with  $p/q \equiv \sqrt{H_{00}/H_{\bar{0}\bar{0}}}$ . The corresponding eigenvalues are

$$\begin{aligned} \lambda_1 &= m_1 - \frac{i}{2}\Gamma_1 = H_{00} + \sqrt{H_{0\bar{0}}H_{\bar{0}0}}, \\ \lambda_2 &= m_2 - \frac{i}{2}\Gamma_2 = H_{00} - \sqrt{H_{0\bar{0}}H_{\bar{0}0}}. \end{aligned} \quad (3)$$

$H$  governs the evolution of the meson state

$$|\psi(t)\rangle = a(t)|M^0\rangle + b(t)|\bar{M}^0\rangle, \quad (4)$$

with

$$\begin{pmatrix} a(t) \\ b(t) \end{pmatrix} = U(t) \begin{pmatrix} a(0) \\ b(0) \end{pmatrix}, \quad (5)$$

where

$$U(t) = \exp(-iHt) = g_+(t) + g_-(t) \begin{pmatrix} 0 & p/q \\ q/p & 0 \end{pmatrix}, \quad (6)$$

with  $g_{\pm}(t) \equiv \frac{e^{-i\lambda_2 t} \pm e^{-i\lambda_1 t}}{2}$ . This leads to the mixing phenomena. Especially,  $M^0$  and  $\bar{M}^0$  at  $t = 0$  evolve respectively to

$$\begin{aligned} |M^0(t)\rangle &= g_+(t)|M^0\rangle + \frac{q}{p}g_-(t)|\bar{M}^0\rangle, \\ |\bar{M}^0(t)\rangle &= \frac{p}{q}g_-(t)|M^0\rangle + g_+(t)|\bar{M}^0\rangle. \end{aligned} \quad (7)$$

For a meson in an arbitrary state, its decay to some final state  $f$  indicates that there has been a projection or filtering to some basis state  $|\phi\rangle$ , which decays to  $f$ ,  $|\phi\rangle$  being [56, 57]

$$|\phi\rangle = \frac{1}{\sqrt{|A_f|^2 + |\bar{A}_f|^2}} \left( \bar{A}_f^* |M^0\rangle + A_f^* |\bar{M}^0\rangle \right), \quad (8)$$

where  $A_f = \langle f|W|M^0\rangle$  and  $\bar{A}_f = \langle f|W|\bar{M}^0\rangle$  are, respectively, the amplitudes of the decays from  $M^0$  and  $\bar{M}^0$  to the final state  $f$ .  $W = \mathcal{U}H_w$ , where  $H_w$  being the weak

decay Hamiltonian while  $\mathcal{U}$  being the strong evolution operator and reducing to the identity if final state interactions are neglected.

A pair of neutral mesons can be produced as  $C = -1$  antisymmetric entangled state

$$|\Psi_{-}\rangle = \frac{1}{\sqrt{2}} \left( |M^0\rangle|\bar{M}^0\rangle - |\bar{M}^0\rangle|M^0\rangle \right), \tag{9}$$

where in each term, the first and second basis states are those of mesons  $a$  and  $b$  respectively.

Suppose this two-particle state evolves up to  $t_a$ , when meson  $a$  decays to some final state  $f_a$ , indicating that there is a projection or filtering of  $a$  to some basis state  $|\phi\rangle_a$ , which decays to  $f_a$ .  $|\phi\rangle_a$  is  $|\phi\rangle$  as given in (8) for meson  $a$ . The meson  $b$  continues to evolve till it decays to some final state  $f_b$  at  $t_b$ , indicating that there is a projection or filtering of  $b$  to some basis state  $|\phi\rangle_b$ , which decays to  $f_b$ .  $|\phi\rangle_b$  is  $|\phi\rangle$  as given in (8) for meson  $b$ . The time evolution of the entangled state up to the projections can be described as  $P_b U_b(t_b - t_a) P_a U_b(t_a) U_a(t_a) |\Psi_{-}\rangle = P_b P_a U(t_b) U(t_a) |\Psi_{-}\rangle = P_b P_a |\Psi_{-}(t_a, t_b)\rangle$ , where  $P_a = |\phi\rangle_{aa}\langle\phi|$  and  $P_b = |\phi\rangle_{bb}\langle\phi|$  are projection operators, and the commutativity between operators on  $a$  and those on  $b$  have been used. This justifies the usual use of a state vector with two time variables

$$\begin{aligned} |\Psi_{-}(t_a, t_b)\rangle &\equiv U(t_b)U(t_a)|\Psi_{-}\rangle \\ &= \frac{1}{\sqrt{2}} \left( |M^0(t_a)\rangle|\bar{M}^0(t_b)\rangle \right. \\ &\quad \left. - |\bar{M}^0(t_a)\rangle|M^0(t_b)\rangle \right), \end{aligned} \tag{10}$$

which means that the two mesons decay at  $t_a$  and  $t_b$ , respectively.

Specifically, we use neutral  $B_d$  mesons, because of the advantage that  $\Gamma_2 \approx \Gamma_1$ ,  $q/p \approx e^{2i\beta}$ , where  $2\beta$  is a phase factor,  $\beta$  is given as  $\sin(2\beta) = 0.695$  [97]. Then  $M^0 = B^0$ ,  $\bar{M}^0 = \bar{B}^0$ ,  $M_1 = B_L$ ,  $M_2 = B_H$ , and  $U(t)$  is simplified to

$$U(t) = e^{-iMt - \frac{\Gamma}{2}t} \times \left( \cos \frac{x\Gamma t}{2} + i \sin \frac{x\Gamma t}{2} \left[ \cos(2\beta)\sigma^x + \sin(2\beta)\sigma^y \right] \right), \tag{11}$$

where  $\sigma^i$ , ( $i = x, y, z$ ), are Pauli operators,  $x \equiv (m_H - m_L)/\Gamma$ ,  $M \equiv (m_H + m_L)/2$  and  $\Gamma \equiv (\Gamma_L + \Gamma_H)/2$ , the subscripts following those of  $B_H$  and  $B_L$ .

In Bloch representation,  $|B^0\rangle$ , like the horizontally polarized state of a photon or the spin-up state of an electron, is represented as the vector  $(0, 0, 1)$ , while  $|\bar{B}_d^0\rangle$ , like the vertically polarized state of a photon or the spin-down state of an electron, is represented as the vector  $(0, 0, -1)$ . They can be chosen as the “measuring directions” or bases of measurement.

However, for a measurement following time evolution, it is more convenient to define an effective time-dependent basis or “measuring direction”. A state of a two-state system can be parameterized as

$$|\mathbf{u}\rangle = e^{i\zeta} \left( \cos \frac{\theta_{\mathbf{u}}}{2} |0\rangle + e^{i\rho_{\mathbf{u}}} \sin \frac{\theta_{\mathbf{u}}}{2} |1\rangle \right), \tag{12}$$

where  $|0\rangle$  and  $|1\rangle$  represent the basis states. We consider its time evolution that can be parameterized as

$$U(\theta_{\mathbf{a}}, \rho_{\mathbf{a}}) = \left( \cos \frac{\theta_{\mathbf{a}}}{2} - i \sin \frac{\theta_{\mathbf{a}}}{2} (\cos(\rho_{\mathbf{a}})\sigma^x + \sin(\rho_{\mathbf{a}})\sigma^y) \right), \tag{13}$$

of which (11) is an example, multiplied by an additional decay factor  $e^{-iMt - \frac{\Gamma}{2}t}$ .

Suppose that following the evolution  $U(\theta_{\mathbf{a}}, \rho_{\mathbf{a}})$ , a signal is recorded as  $\mathcal{A} = +1$  if  $|0\rangle$  is detected, while  $\mathcal{A} = -1$  if  $|1\rangle$  is detected. The QM expectation value of  $\mathcal{A}$  is

$$\bar{\mathcal{A}}(\mathbf{u}) = \frac{|0|U|\mathbf{u}\rangle|^2 - |1|U|\mathbf{u}\rangle|^2}{|0|U|\mathbf{u}\rangle|^2 + |1|U|\mathbf{u}\rangle|^2} = \mathbf{u} \cdot \mathbf{a}, \tag{14}$$

where

$$\mathbf{u} = (\sin \theta_{\mathbf{u}} \cos \rho_{\mathbf{u}}, \sin \theta_{\mathbf{u}} \sin \rho_{\mathbf{u}}, \cos \theta_{\mathbf{u}}) \tag{15}$$

is the Bloch vector of  $|\mathbf{u}\rangle$ , while

$$\mathbf{a} = (-\sin \theta_a \sin \rho_a, \sin \theta_a \cos \rho_a, \cos \theta_a) \tag{16}$$

is the Bloch vector of  $U^\dagger(\theta_{\mathbf{a}}, \rho_{\mathbf{a}})|0\rangle$ . This can be easily understood by regarding  $\bar{\mathcal{A}}(\mathbf{u})$  as expectation value of the signal obtained by measuring the initial state  $|\mathbf{u}\rangle$  in the rotated basis  $\{U^\dagger|0\rangle, U^\dagger|1\rangle\}$ . The rotation  $U^\dagger$  of the basis is realized by evolution.

For a  $B_d$  meson, the measurement in the flavor basis  $\{|B^0\rangle, |\bar{B}^0\rangle\}$ , corresponding to  $\mathcal{A}_l = \pm 1$ , can be made through the semileptonic decay channel, as the direct CP violation or wrong sign decay is negligible [97]. Thus  $|\phi\rangle$  in (8) reduces to  $|B^0\rangle$  or  $|\bar{B}^0\rangle$ , and one can define

$$\bar{\mathcal{A}}_l(\mathbf{u}) = \frac{|B^0|U(t)|\mathbf{u}\rangle|^2 - |\bar{B}^0|U(t)|\mathbf{u}\rangle|^2}{|B^0|U(t)|\mathbf{u}\rangle|^2 + |\bar{B}^0|U(t)|\mathbf{u}\rangle|^2} = \mathbf{u} \cdot \mathbf{a}^l(t), \tag{17}$$

where

$$\mathbf{a}^l(t) = (\sin(2\beta) \sin(x\Gamma t), -\cos(2\beta) \sin(x\Gamma t), \cos(x\Gamma t)).$$

Likewise, as the direct CP violation is negligible [97], if the decay products are CP eigenstates  $S_{\pm}$ , they signals the projection of the meson to CP basis states  $|B_{\pm}\rangle \equiv (|B^0\rangle \pm |\bar{B}^0\rangle)/\sqrt{2}$ . In this case,  $|\phi\rangle$  in (8) reduces to  $|B_{\pm}\rangle$ .

With  $B_{\pm}$  corresponding to  $\mathcal{A}_s = \pm 1$ , one can define

$$\bar{\mathcal{A}}_s(\mathbf{u}) = \frac{|\langle B_+ | U(t) | \mathbf{u} \rangle|^2 - |\langle B_- | U(t) | \mathbf{u} \rangle|^2}{|\langle B_+ | U(t) | \mathbf{u} \rangle|^2 + |\langle B_- | U(t) | \mathbf{u} \rangle|^2} = \mathbf{u} \cdot \mathbf{a}^s(t), \tag{18}$$

where

$$\mathbf{a}^s(t) = \left( \sin^2(2\beta) \cos(x\Gamma t) + \cos^2(2\beta), \right. \\ \left. \sin(4\beta) \sin^2(x\Gamma t/2), -\sin(2\beta) \sin(x\Gamma t) \right).$$

Equations (17) and (18) are of the same form as the standard QM result (14) because the factor  $e^{-\Gamma t}$  exists in all terms in both denominator and the numerator, and thus cancels.

Note that  $|\langle B^0 | U(t) | \mathbf{u} \rangle|^2$ ,  $|\langle \bar{B}^0 | U(t) | \mathbf{u} \rangle|^2$  and  $|\langle B_{\pm} | U(t) | \mathbf{u} \rangle|^2$  do not depend on the specific decay channels signalling the projection, hence is not directly observed. In contrast CP asymmetries usually defined depend on which channels are observed.

However, under the assumption of no wrong sign decays and no direct CP violation,  $|\langle B^0 | U(t) | \mathbf{u} \rangle|^2$ ,  $|\langle \bar{B}^0 | U(t) | \mathbf{u} \rangle|^2$  and  $|\langle B_{\pm} | U(t) | \mathbf{u} \rangle|^2$  and thus the asymmetries we define above are related to the rates of decays in specific channels. For flavor eigenstates  $l^{\pm}$ , as the final states of semileptonic decays,

$$\langle l^+ | W U(t) | \mathbf{u} \rangle = \langle l^+ | W | B^0 \rangle \langle B^0 | U(t) | \mathbf{u} \rangle = A_{l^+} \langle B^0 | U(t) | \mathbf{u} \rangle, \\ \langle l^- | W U(t) | \mathbf{u} \rangle = \langle l^- | W | \bar{B}^0 \rangle \langle \bar{B}^0 | U(t) | \mathbf{u} \rangle = \bar{A}_{l^-} \langle \bar{B}^0 | U(t) | \mathbf{u} \rangle.$$

For  $|l^-\rangle = CP|l^+\rangle$ , we have  $A_{l^+} = \bar{A}_{l^-} = A_l$ . For CP eigenstates  $S_{\pm}$  as the final states,

$$\langle S_+ | W U(t) | \mathbf{u} \rangle = \langle S_+ | W | B_+ \rangle \langle B_+ | U(t) | \mathbf{u} \rangle, \\ \langle S_- | W U(t) | \mathbf{u} \rangle = \langle S_- | W | B_- \rangle \langle B_- | U(t) | \mathbf{u} \rangle.$$

Note that here there is no special relation between  $l^+$  and  $l^-$ , or between  $S_+$  and  $S_-$ , as different decay channels may signal a same projection in the meson Hilbert space. The examples of flavor eigenstates  $l^{\pm}$  as the final states include  $M^- e^+ \nu$ ,  $M^+ e^- \bar{\nu}$ ,  $M^- \mu^+ \nu$ ,  $M^+ \mu^- \bar{\nu}$ , etc. The examples of CP eigenstates  $S_{\pm}$  as the final states include  $J/\psi K_S$ ,  $J/\psi K_L$ ,  $KK$ ,  $KKK$ ,  $\pi\pi$ ,  $\pi\pi\pi$ ,  $DD$ , etc.

Therefore, the asymmetries  $\bar{A}_l$  and  $\bar{A}_s$ , defined above in the meson Hilbert space, can be obtained from experimentally measurable quantities,

$$\bar{\mathcal{A}}_l(\mathbf{u}) = \frac{\frac{|\langle l^+ | W U(t) | \mathbf{u} \rangle|^2}{|\langle l^+ | W | B^0 \rangle|^2} - \frac{|\langle l^- | W U(t) | \mathbf{u} \rangle|^2}{|\langle l^- | W | \bar{B}^0 \rangle|^2}}{\frac{|\langle l^+ | W U(t) | \mathbf{u} \rangle|^2}{|\langle l^+ | W | B^0 \rangle|^2} + \frac{|\langle l^- | W U(t) | \mathbf{u} \rangle|^2}{|\langle l^- | W | \bar{B}^0 \rangle|^2}},$$

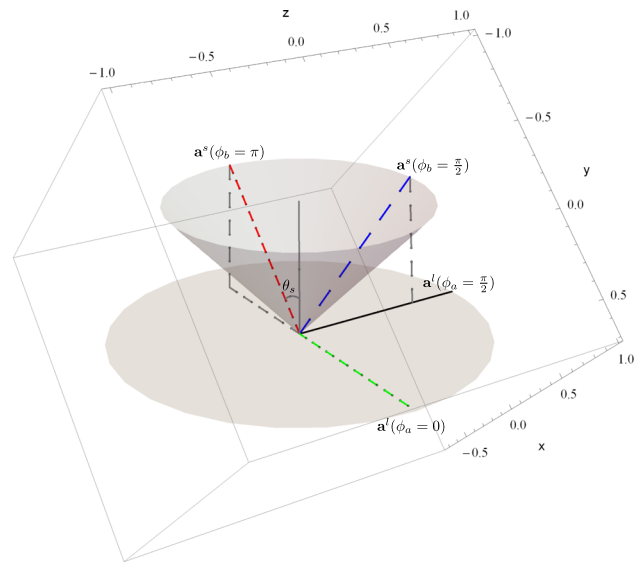


**Fig. 1** The effective measuring directions  $\mathbf{a}^l$  and  $\mathbf{a}^s$ . In a certain coordinate system,  $\mathbf{a}^l(\phi_l)$  is on  $xy$  plane,  $\mathbf{a}^s(\theta_s, \phi_s)$  is on a cone. For  $B_d$  mesons,  $\phi_l = x\Gamma t$ ,  $(\phi_s, \theta_s) = (x\Gamma t + \pi/2, 2\beta)$ , corresponding to flavor and CP measurements following evolution of time  $t$ , respectively. For photon polarizations,  $\mathbf{a}^l$  and  $\mathbf{a}^s$  are polarizer directions in Bloch representation, and can be adjusted directly

$$\bar{\mathcal{A}}_s(\mathbf{u}) = \frac{\frac{|\langle S_+ | W U(t) | \mathbf{u} \rangle|^2}{|\langle S_+ | W | B_+ \rangle|^2} - \frac{|\langle S_- | W U(t) | \mathbf{u} \rangle|^2}{|\langle S_- | W | B_- \rangle|^2}}{\frac{|\langle S_+ | W U(t) | \mathbf{u} \rangle|^2}{|\langle S_+ | W | B_+ \rangle|^2} + \frac{|\langle S_- | W U(t) | \mathbf{u} \rangle|^2}{|\langle S_- | W | B_- \rangle|^2}}.$$

As shown in Fig. 1, with the time passing,  $\mathbf{a}^l(t)$  rotates on a plane, while  $\mathbf{a}^s(t)$  rotates on a cone whose axis is perpendicular to  $\mathbf{a}^l$  plane. For convenience, we adopt a new coordinate system in which  $\mathbf{a}^l$  plane is the  $xy$  plane, then

$$\mathbf{a}^l(\phi_l) = (\cos \phi_l, \sin \phi_l, 0), \\ \mathbf{a}^s(\theta_s, \phi_s) = (\sin \theta_s \cos \phi_s, \sin \theta_s \sin \phi_s, \cos \theta_s), \tag{19}$$

where  $\phi_l = x\Gamma t$  and  $\phi_s = x\Gamma t + \pi/2$  are the azimuthal angles of  $\mathbf{a}^l$  and  $\mathbf{a}^s$ , respectively,  $\theta_s = 2\beta$  is the polar angle of  $\mathbf{a}^s$ , and it suffices to consider  $0 < \theta_s \leq \pi/2$ .

$\mathbf{a}^l(\phi_l)$  and  $\mathbf{a}^s(\theta_s, \phi_s)$  are two effective measurement settings or “measuring directions”. For  $B_d$  mesons, they are time-dependent. The rotation of basis or measuring direction realized by evolution explains the similarity between decay time and polarizer angle. But  $\mathbf{a}^l(\phi_l)$  and  $\mathbf{a}^s(\theta_s, \phi_s)$  can also be used, say, for photon polarization, by directly adjusting  $\phi_l$  and  $(\theta_s, \phi_s)$  in experiments.

### 3 CNHV theories

$|\mathbf{u}\rangle$  is an eigenstate of the Pauli operator  $\boldsymbol{\sigma} \cdot \mathbf{u}$  in the direction of  $\mathbf{u}$ . A particle in this state has a definite  $\mathbf{u}$ . For a single particle, QM result can be reproduced by a realistic or HV theory, in which the measurement outcomes are determined by preexisting properties independent of the measurement, or “elements of reality” in the words of EPR. Thus  $\mathbf{u}$  is identified as such an element of reality.

Consider a HV theory. Suppose a particle with property  $\mathbf{u}$  is measured along direction  $\mathbf{a}$ , then the dichotomic measurement outcome  $A = \pm 1$  is determined by the hidden variables  $\lambda$  in addition to the property  $\mathbf{u}$  and the local parameter  $\mathbf{a}$ . This is also called a local realistic theory, in which the parameter  $\mathbf{a}$  is local. In a nonlocal realistic theory,  $A$  also depends on a non-local parameters, collectively denoted as  $\eta$ . In a cryptononlocal HV (CNHV) theory, the individual properties of each particle, after averaging over distribution  $\rho_{\mathbf{u}}(\lambda)$  of the hidden variables  $\lambda$ , become local, as indicated in countless phenomena,

$$\int d\lambda \rho_{\mathbf{u}}(\lambda) A(\mathbf{u}, \mathbf{a}, \eta, \lambda) = \bar{A}(\mathbf{u}, \mathbf{a}). \tag{20}$$

A concrete example of  $\bar{A}(\mathbf{u}, \mathbf{a})$  is the Malus’ law [16]

$$\bar{A}(\mathbf{u}, \mathbf{a}) = \mathbf{u} \cdot \mathbf{a}, \tag{21}$$

which is consistent with QM results of photon polarizations. In the last section, we have just shown that it is also consistent with QM result of the meson decay following its evolution.

For a pair of particles from a common source, with respective properties  $\mathbf{u}$  and  $\mathbf{v}$ , the measuring direction of the other particle can serve as the nonlocal parameter, and one can also assume nonlocal parameters  $\eta_a$  and  $\eta_b$ , which are nonlocal with respect to  $\mathbf{a}$  and  $\mathbf{b}$ , respectively. The measurement outcomes along respective directions  $\mathbf{a}$  and  $\mathbf{b}$  are  $A(\mathbf{u}, \mathbf{v}, \mathbf{a}, \mathbf{b}, \eta_a, \eta_b, \lambda) = \pm 1$  and  $B(\mathbf{v}, \mathbf{u}, \mathbf{b}, \mathbf{a}, \eta_b, \eta_a, \lambda) = \pm 1$ . The local measurement of each particle cannot detect its correlation with the other particle, hence the nonlocal dependence disappears after averaging over the hidden variables,

$$\int d\lambda \rho_{\mathbf{u}, \mathbf{v}}(\lambda) A(\mathbf{u}, \mathbf{v}, \mathbf{a}, \mathbf{b}, \eta_a, \eta_b, \lambda) = \bar{A}(\mathbf{u}, \mathbf{a}), \tag{22}$$

$$\int d\lambda \rho_{\mathbf{u}, \mathbf{v}}(\lambda) B(\mathbf{v}, \mathbf{u}, \mathbf{b}, \mathbf{a}, \eta_b, \eta_a, \lambda) = \bar{B}(\mathbf{v}, \mathbf{b}). \tag{23}$$

A general physical state is a statistical mixture of subensembles with definite  $\mathbf{u}$  and  $\mathbf{v}$ . Hence the final expectation values, which is experimentally measured, are [15, 16]

$$\begin{aligned} \langle A \rangle &= \int d\mathbf{u} F(\mathbf{u}) \bar{A}(\mathbf{u}), \\ \langle B \rangle &= \int d\mathbf{v} F(\mathbf{v}) \bar{B}(\mathbf{v}), \end{aligned} \tag{24}$$

where  $F(\mathbf{u})$  and  $F(\mathbf{v})$  are probability distribution of polarizations  $\mathbf{u}$  and  $\mathbf{v}$ , respectively. In case of correlated particles,

they are the reduced ones

$$\begin{aligned} F(\mathbf{u}) &= \int d\mathbf{v} F(\mathbf{u}, \mathbf{v}), \\ F(\mathbf{v}) &= \int d\mathbf{u} F(\mathbf{u}, \mathbf{v}). \end{aligned} \tag{25}$$

The two-body quantities may indicate correlations. For definite  $\mathbf{u}$  and  $\mathbf{v}$ ,

$$\begin{aligned} \overline{AB}(\mathbf{u}, \mathbf{v}, \mathbf{a}, \mathbf{b}) &= \int d\lambda \rho_{\mathbf{u}, \mathbf{v}}(\lambda) A(\mathbf{u}, \mathbf{v}, \mathbf{a}, \mathbf{b}, \lambda) \\ &B(\mathbf{v}, \mathbf{u}, \mathbf{b}, \mathbf{a}, \lambda). \end{aligned} \tag{26}$$

For a general state,

$$E(\mathbf{a}, \mathbf{b}) = \int d\mathbf{u} d\mathbf{v} F(\mathbf{u}, \mathbf{v}) \overline{AB}(\mathbf{u}, \mathbf{v}, \mathbf{a}, \mathbf{b}), \tag{27}$$

which is the main quantity to be investigated, as it may differ with the corresponding QM result when entanglement is present, in which case a probability distribution over subensembles with definite polarizations leads to inequalities violated by the entangled state in QM.

Here we extend CNHV theories to include the case that  $\mathbf{a}$  and  $\mathbf{b}$  are not externally fixed. In each measurement, the measurement settings  $\tilde{\mathbf{a}}(\lambda)$  and  $\tilde{\mathbf{b}}(\lambda)$  are determined by HV  $\lambda$ , thus the measurement outcomes are like  $A(\mathbf{u}, \tilde{\mathbf{a}}(\lambda), \eta, \lambda)$ . Nevertheless, for those measurements with  $\tilde{\mathbf{a}}(\lambda) = \mathbf{a}$ , we can obtain the average of the outcomes. In the case of a single particle, the average is

$$\int d\lambda \rho'_{\mathbf{u}, \mathbf{a}}(\lambda) A(\mathbf{u}, \tilde{\mathbf{a}}(\lambda), \eta, \lambda) = \bar{A}(\mathbf{u}, \mathbf{a}) = \mathbf{u} \cdot \mathbf{a}, \tag{28}$$

where  $\rho'_{\mathbf{u}, \mathbf{a}}(\lambda) \equiv \rho_{\mathbf{u}}(\lambda) \delta(\tilde{\mathbf{a}}(\lambda) - \mathbf{a})$  is a shorthand.

Likewise, for two correlated particles, the outcomes of those measurements with  $\tilde{\mathbf{a}}(\lambda) = \mathbf{a}$  and  $\tilde{\mathbf{b}}(\lambda) = \mathbf{b}$  give rise to

$$\begin{aligned} &\int d\lambda \rho_{\mathbf{u}, \mathbf{v}}(\lambda) \delta(\tilde{\mathbf{a}}(\lambda) - \mathbf{a}) \delta(\tilde{\mathbf{b}}(\lambda) - \mathbf{b}) \\ &\quad \times A(\mathbf{u}, \mathbf{v}, \tilde{\mathbf{a}}(\lambda), \tilde{\mathbf{b}}(\lambda), \eta_a, \eta_b, \lambda) \\ &= \bar{A}(\mathbf{u}, \mathbf{a}) = \mathbf{u} \cdot \mathbf{a}, \end{aligned} \tag{29}$$

$$\begin{aligned} &\int d\lambda \rho_{\mathbf{u}, \mathbf{v}}(\lambda) \delta(\tilde{\mathbf{a}}(\lambda) - \mathbf{a}) \delta(\tilde{\mathbf{b}}(\lambda) - \mathbf{b}) \\ &\quad \times B(\mathbf{v}, \mathbf{u}, \tilde{\mathbf{b}}(\lambda), \tilde{\mathbf{a}}(\lambda), \eta_b, \eta_a, \lambda) \\ &= \bar{B}(\mathbf{v}, \mathbf{b}) = \mathbf{v} \cdot \mathbf{b}. \end{aligned} \tag{30}$$

$$\begin{aligned} \overline{AB}(\mathbf{u}, \mathbf{v}, \mathbf{a}, \mathbf{b}) &= \int d\lambda \rho_{\mathbf{u}, \mathbf{v}}(\lambda) \delta(\tilde{\mathbf{a}}(\lambda) - \mathbf{a}) \delta(\tilde{\mathbf{b}}(\lambda) - \mathbf{b}) \\ &\quad \times A(\mathbf{u}, \mathbf{v}, \tilde{\mathbf{a}}(\lambda), \tilde{\mathbf{b}}(\lambda), \eta_a, \eta_b, \lambda) \\ &\quad B(\mathbf{v}, \mathbf{u}, \tilde{\mathbf{b}}(\lambda), \tilde{\mathbf{a}}(\lambda), \eta_b, \eta_a, \lambda). \end{aligned} \tag{31}$$

Clearly the original formalism is a special case of this extension, by externally fixing  $\tilde{\mathbf{a}}(\lambda)$  to be always  $\mathbf{a}$  and  $\tilde{\mathbf{b}}(\lambda)$  to be always  $\mathbf{b}$ , independent of  $\lambda$ .

#### 4 LI for measuring directions on a plane and a cone

We now consider a pair of particles  $a$  and  $b$ , with the measurement outcomes  $A = \pm 1$  and  $B = \pm 1$ , respectively. The average of those outcomes  $A$  with a same measurement setting  $\mathbf{a}$  satisfy the Malus' Law (29). The average of those outcomes  $B$  with a same measurement setting  $\mathbf{b}$  satisfy the Malus' Law (30). The correlation function is defined in the way of (31).  $\mathbf{a}$  and  $\mathbf{b}$  are each given as  $\mathbf{a}^l(\phi_i)$  or  $\mathbf{a}^s(\theta_s, \phi_i)$ , ( $i = a, b$ ), as in (19).

We first consider correlation functions of various combinations of  $\mathbf{a}^l$  and  $\mathbf{a}^s$ . Define  $\hat{E}^\pm(\mathbf{a}, \mathbf{b}) \equiv E(\mathbf{a}, \mathbf{b}) + E(\mathbf{b}, \pm\mathbf{a})$ , and rewrite  $\hat{E}^\pm(\mathbf{a}^s(\theta_s, \phi_a), \mathbf{a}^l(\phi_b))$  as  $\hat{E}_{sl}^\pm(\theta_s, \xi, \varphi)$ , where  $\xi \equiv (\phi_a + \phi_b)/2$ ,  $\varphi \equiv \phi_a - \phi_b$ .  $\hat{E}_{ll}^\pm(\theta_s, \xi, \varphi)$  and  $\hat{E}_{ss}^\pm(\theta_s, \xi, \varphi)$  are similarly defined. Furthermore, we consider the averages over  $\xi$ ,  $\hat{E}_{sl}^-(\theta_s, \varphi) \equiv \int \frac{d\xi}{2\pi} \hat{E}_{sl}^-(\theta_s, \xi, \varphi)$  and so on.

In the Appendix, we prove the following LI. The upper bound is given by

$$\begin{aligned} & \hat{E}_{sl}^-(\theta_s, \varphi_1) + \frac{\pi \cos(\theta_1(\theta_s, \varphi_1))L_1(\theta_s, \varphi_1)}{4 \cos(\frac{\varphi_2}{2})} \hat{E}_{ll}^-(\theta_s, \varphi_2) \\ & \leq 2 \left( 1 + \frac{\pi \cos(\theta_1(\theta_s, \varphi_1))L_1(\theta_s, \varphi_1)}{4 \cos(\frac{\varphi_2}{2})} \right) \\ & \quad - \cos(\theta_1(\theta_s, \varphi_1))L_1(\theta_s, \varphi_1), \end{aligned} \tag{32}$$

where

$$\begin{aligned} L_1(\theta_s, \varphi) & \equiv |\mathbf{a}^s + \mathbf{a}^l| = \sqrt{2 + 2 \cos(\varphi) \sin(\theta_s)}, \\ \theta_1(\theta_s, \varphi) & = \cos^{-1} \frac{\cos(\theta_s)}{\sqrt{2 + 2 \cos(\varphi) \sin(\theta_s)}}. \end{aligned}$$

With  $0 < \theta_s < \pi/2$ , we have  $\sin(\theta_1) > 0$ ,  $\cos(\theta_1) > 0$ .

We find two lower bounds. The first is given as

$$\begin{aligned} & \hat{E}_{sl}^+(\theta_s, \varphi_1) + \frac{\pi \cos(\theta_2(\theta_s, \varphi_1))L_2(\theta_s, \varphi_1)}{4 |\sin(\frac{\varphi_2}{2})|} \hat{E}_{ll}^+(\theta_s, \varphi_2) \\ & \geq -2 \left( 1 + \frac{\pi \cos(\theta_2(\theta_s, \varphi_1))L_2(\theta_s, \varphi_1)}{4 |\sin(\frac{\varphi_2}{2})|} \right) \\ & \quad + \cos(\theta_2(\theta_s, \varphi_1))L_2(\theta_s, \varphi_1). \end{aligned} \tag{33}$$

where

$$\begin{aligned} L_2(\theta_s, \varphi) & \equiv |\mathbf{a}^s - \mathbf{a}^l| = \sqrt{2 - 2 \cos(\varphi) \sin(\theta_s)}, \\ \theta_2(\theta_s, \varphi) & = \cos^{-1} \frac{\cos(\theta_s)}{\sqrt{2 - 2 \cos(\varphi) \sin(\theta_s)}}. \end{aligned}$$

The second lower bound is given as

$$\hat{E}_{sl}^+(\theta_s, \varphi_1) + \frac{\pi \cos(\theta_2(\theta_s, \varphi_1))L_2(\theta_s, \varphi_1)}{4 \sin(\theta_s) |\sin(\frac{\varphi_2}{2})|} \hat{E}_{ss}^+(\varphi_2)$$

$$\begin{aligned} & \geq -2 \left( 1 + \frac{\pi \cos(\theta_2(\theta_s, \varphi_1))L_2(\theta_s, \varphi_1)}{4 \sin(\theta_s) |\sin(\frac{\varphi_2}{2})|} \right) \\ & \quad + \cos(\theta_2)L_2(\theta_s, \varphi_1). \end{aligned} \tag{34}$$

Equations (32), (33) and (34) comprise our LI.

The correlation functions averaged over  $\xi$  are not directly observable, therefore rotational invariance or fair sampling of the averages needs to be assumed for measurements, in order that LI in terms of these average correlation functions can be experimentally examined [17,18]. In the case of meson decays, the rotational invariance in Bloch representation is actually time translational invariance.

To drop this additional assumption, we can redefine each average in a discrete way,

$$\hat{E}_{sl}^\pm(\theta_s, \varphi) \equiv \frac{1}{N} \sum_{n=1}^N \hat{E}_{sl}^\pm \left( \theta_s, \xi_n = \frac{2n\pi}{N}, \varphi \right), \tag{35}$$

and  $\hat{E}_{ll}^\pm(\theta_s, \varphi)$  and  $\hat{E}_{ss}^\pm(\theta_s, \varphi)$  similarly. As derived in the Appendix, for these discrete average correlation functions, our LI can be obtained from Eqs. (32), (33) and (34) by simply replacing  $\pi/4$  as  $1/2u_N$ , where  $u_N \equiv \frac{1}{N} \cot(\frac{\pi}{2N})$ .  $N \geq 2$  is required. As  $N \rightarrow \infty$ ,  $u_N \rightarrow 2/\pi$ , then the discrete version approaches the continuous version.

Our LI can be tested using various systems, in which measurement directions  $\mathbf{a}^l(\phi_l)$  and  $\mathbf{a}^s(\theta_s, \phi_s)$  can be directly adjusted.

For meson decays,  $\theta_s = 2\beta$  is fixed, while  $\phi_l = \phi_l(t) = x\Gamma t$ ,  $\phi_s = \phi_s(t) = x\Gamma t + \frac{\pi}{2}$  are given by the decay time  $t$ . We mention that for the two particles  $a$  and  $b$  to be separated in spacelike distance, there is a constraint on the decay times  $t_a$  and  $t_b$ . Suppose the particle pairs are generated from a particle at rest and each flies in velocity  $v$  to opposite directions. Then spacelike separation means  $(1 + w)t_a > (1 - w)t_b$ , where  $w = (v/c)/\sqrt{1 - v^2/c^2}$ . Consequently there is a constraint on possible values of  $\xi$ , but it does not affect the averages over  $\xi$ , which is an angle mathematically, hence its functions are periodic.

#### 5 Testing LI in entangled $B_d$ mesons

We now come back to the  $C = -1 B^0 \bar{B}^0$  entangled meson pairs, and we can write the correlation functions as

$$E(\mathbf{a}^X(t_a), \mathbf{a}^Y(t_b)), (X, Y = l, s).$$

By definition,

$$\begin{aligned} & E(\mathbf{a}^X(t_a), \mathbf{a}^Y(t_b)) \\ & = [(P(X+, Y+, t_a, t_b) + P(X-, Y-, t_a, t_b) \\ & \quad - P(X+, Y-, t_a, t_b) - P(X-, Y+, t_a, t_b)]/ \end{aligned}$$

$$[P(X+, Y+, t_a, t_b) + P(X-, Y-, t_a, t_b) + P(X+, Y-, t_a, t_b) + P(X-, Y+, t_a, t_b)], \tag{36}$$

where for convenience, we have invented the shorthand

$$l+ \equiv B^0, \quad l- \equiv \bar{B}^0, \quad s\pm \equiv B_{\pm}, \tag{37}$$

which should not be confused with  $l^{\pm}$  and  $S_{\pm}$ , with  $\pm$  as the superscript or subscript, denoting the final states of decays.

$P(X\pm, Y\pm, t_a, t_b)$  is the probability that the measurement results of a and b are  $X\pm$  and  $Y\pm$  at  $t_a$  and  $t_b$ , respectively, indicated by the final states of their respective decays. The measurement or filtering or projection in the flavor basis  $\{B^0, \bar{B}^0\}$  is made through a semileptonic decay to a flavor eigenstate  $|l^{\pm}\rangle$ . The measurement or filtering or projection in CP basis  $\{B_+, B_-\}$  is made through a decay into CP eigenstate  $|S_{\pm}\rangle$ . With direct CP violation negligible, we have  $A_{l-} = \bar{A}_{l+} = 0, A_{S_{\pm}} = \pm \bar{A}_{S_{\pm}}$ . Only if  $|l^- \rangle = CP|l^+ \rangle$ , we have  $A_{l+} = \bar{A}_{l-}$ . Note that the decay products of a and b may be different even though their flavor or CP eigenvalues are the same, and may not be CP conjugates even though their flavor eigenvalues are opposites.

The basis of measurement, namely flavor or CP basis, is not actively chosen by experiments, but is signalled by the decay products. Our extension of CNHV and LI addresses this issue, as the main achievement of this paper.

A key quantity is the joint decay rate for particle a decaying to  $f_a$  at  $t_a$  while particle b decaying to  $f_b$  at  $t_b$ ,  $R(f_a, f_b, t_a, t_b) \propto |\langle f_a, f_b | W_a W_b | \Psi(t_a, t_b) \rangle|^2$ . The following joint decay amplitudes will be needed.

There are four amplitudes in the form of

$$\langle l_a^{\pm}, l_b^{\pm} | W_a W_b | \Psi(t_a, t_b) \rangle = A_{l_a^{\pm}} A_{l_b^{\pm}} \langle l_{\pm}, l_{\pm} | \Psi(t_a, t_b) \rangle, \tag{38}$$

where,  $\pm$  in  $l_a^{\pm}$  corresponds to the first  $l\pm$  on RHS,  $\pm$  in  $l_b^{\pm}$  corresponds to the second  $l\pm$  on RHS.

There are four amplitudes of the form of

$$\langle S_{\pm}^a, S_{\pm}^b | W_a W_b | \Psi(t_a, t_b) \rangle = 2A_{S_{\pm}^a} A_{S_{\pm}^b} \langle s_{\pm}, s_{\pm} | \Psi(t_a, t_b) \rangle, \tag{39}$$

where we have used  $\langle S_{\pm} | W | B_{\pm} \rangle = (A_{S_{\pm}} \pm \bar{A}_{S_{\pm}}) / \sqrt{2} = \sqrt{2} A_{S_{\pm}}$ .

There are four other amplitudes of the form of

$$\langle S_{\pm}^a, l_b^{\pm} | W_a W_b | \Psi(t_a, t_b) \rangle = \sqrt{2} A_{S_{\pm}^a} A_{l_b^{\pm}} \langle s_{\pm}, l_{\pm} | W_a W_b | \Psi(t_a, t_b) \rangle. \tag{40}$$

The experimentally measured quantity is the number of the joint events  $N(f_a, f_b, t_a, t_b) \propto \epsilon_{f_a, f_b} R(f_a, f_b, t_a, t_b)$ , where  $\epsilon_{f_a, f_b}$  is the detection efficiency for that channel [49],  $R(f_a, f_b, t_a, t_b)$  is proportional to the modulo square of the joint decay amplitude, as given in Eqs. (38–40).

Therefore the correlation function (36) can be obtained from event numbers as

$$E(\mathbf{a}^l(t_a), \mathbf{a}^l(t_b)) = \left( \frac{N(l_a^+, l_b^+, t_a, t_b)}{\epsilon_{l_a^+, l_b^+} |A_{l_a^+}|^2 |A_{l_b^+}|^2} + \frac{N(l_a^-, l_b^-, t_a, t_b)}{\epsilon_{l_a^-, l_b^-} |\bar{A}_{l_a^-}|^2 |\bar{A}_{l_b^-}|^2} - \frac{N(l_a^+, l_b^-, t_a, t_b)}{\epsilon_{l_a^+, l_b^-} |A_{l_a^+}|^2 |\bar{A}_{l_b^-}|^2} - \frac{N(l_a^-, l_b^+, t_a, t_b)}{\epsilon_{l_a^-, l_b^+} |\bar{A}_{l_a^-}|^2 |A_{l_b^+}|^2} \right) / \left( \frac{N(l_a^+, l_b^+, t_a, t_b)}{\epsilon_{l_a^+, l_b^+} |A_{l_a^+}|^2 |A_{l_b^+}|^2} + \frac{N(l_a^-, l_b^-, t_a, t_b)}{\epsilon_{l_a^-, l_b^-} |\bar{A}_{l_a^-}|^2 |\bar{A}_{l_b^-}|^2} + \frac{N(l_a^+, l_b^-, t_a, t_b)}{\epsilon_{l_a^+, l_b^-} |A_{l_a^+}|^2 |\bar{A}_{l_b^-}|^2} + \frac{N(l_a^-, l_b^+, t_a, t_b)}{\epsilon_{l_a^-, l_b^+} |\bar{A}_{l_a^-}|^2 |A_{l_b^+}|^2} \right), \tag{41}$$

$$E(\mathbf{a}^s(t_a), \mathbf{a}^l(t_b)) = \left( \frac{N(S_a^+, l_b^+, t_a, t_b)}{\epsilon_{S_a^+, l_b^+} |A_{S_a^+}|^2 |A_{l_b^+}|^2} + \frac{N(S_a^-, l_b^-, t_a, t_b)}{\epsilon_{S_a^-, l_b^-} |A_{S_a^-}|^2 |\bar{A}_{l_b^-}|^2} - \frac{N(S_a^+, l_b^-, t_a, t_b)}{\epsilon_{S_a^+, l_b^-} |A_{S_a^+}|^2 |\bar{A}_{l_b^-}|^2} - \frac{N(S_a^-, l_b^+, t_a, t_b)}{\epsilon_{S_a^-, l_b^+} |A_{S_a^-}|^2 |A_{l_b^+}|^2} \right) / \left( \frac{N(S_a^+, l_b^+, t_a, t_b)}{\epsilon_{S_a^+, l_b^+} |A_{S_a^+}|^2 |A_{l_b^+}|^2} + \frac{N(S_a^-, l_b^-, t_a, t_b)}{\epsilon_{S_a^-, l_b^-} |A_{S_a^-}|^2 |\bar{A}_{l_b^-}|^2} + \frac{N(S_a^+, l_b^-, t_a, t_b)}{\epsilon_{S_a^+, l_b^-} |A_{S_a^+}|^2 |\bar{A}_{l_b^-}|^2} + \frac{N(S_a^-, l_b^+, t_a, t_b)}{\epsilon_{S_a^-, l_b^+} |A_{S_a^-}|^2 |A_{l_b^+}|^2} \right), \tag{42}$$

$$E(\mathbf{a}^s(t_a), \mathbf{a}^s(t_b)) = \left( \frac{N(S_a^+, S_b^+, t_a, t_b)}{\epsilon_{S_a^+, S_b^+} |A_{S_a^+}|^2 |A_{S_b^+}|^2} + \frac{N(S_a^-, S_b^-, t_a, t_b)}{\epsilon_{S_a^-, S_b^-} |A_{S_a^-}|^2 |A_{S_b^-}|^2} - \frac{N(S_a^+, S_b^-, t_a, t_b)}{\epsilon_{S_a^+, S_b^-} |A_{S_a^+}|^2 |A_{S_b^-}|^2} - \frac{N(S_a^-, S_b^+, t_a, t_b)}{\epsilon_{S_a^-, S_b^+} |A_{S_a^-}|^2 |A_{S_b^+}|^2} \right) / \left( \frac{N(S_a^+, S_b^+, t_a, t_b)}{\epsilon_{S_a^+, S_b^+} |A_{S_a^+}|^2 |A_{S_b^+}|^2} + \frac{N(S_a^-, S_b^-, t_a, t_b)}{\epsilon_{S_a^-, S_b^-} |A_{S_a^-}|^2 |A_{S_b^-}|^2} + \frac{N(S_a^+, S_b^-, t_a, t_b)}{\epsilon_{S_a^+, S_b^-} |A_{S_a^+}|^2 |A_{S_b^-}|^2} + \frac{N(S_a^-, S_b^+, t_a, t_b)}{\epsilon_{S_a^-, S_b^+} |A_{S_a^-}|^2 |A_{S_b^+}|^2} \right), \tag{43}$$

where  $\epsilon$ 's are the detection efficiencies. In experiments,  $|A_{l_i^{\pm}}|^2$  and  $|A_{S_i^{\pm}}|^2$ , ( $i = a, b$ ), can be absorbed to the redefinitions of detection efficiencies.

Furthermore, one obtains

$$\hat{E}^{ll\pm}(\phi_a, \phi_b) \equiv E(\mathbf{a}^l(x\Gamma t_a), \mathbf{a}^l(x\Gamma t_b))$$

$$\begin{aligned}
 &+ E\left(\mathbf{a}^l(x\Gamma t_b), \pm \mathbf{a}^l(x\Gamma t_b)\right), \\
 \hat{E}^{sl\pm}(\phi_a, \phi_b) &\equiv E\left(\mathbf{a}^s\left(x\Gamma t_a + \frac{\pi}{2}\right), \mathbf{a}^l(x\Gamma t_b)\right) \\
 &+ E\left(\mathbf{a}^l(x\Gamma t_b), \pm \mathbf{a}^l(x\Gamma t_b)\right), \\
 \hat{E}_{ss}^+(\phi_a, \phi_b) &\equiv E\left(\mathbf{a}^s\left(x\Gamma t_a + \frac{\pi}{2}\right), \mathbf{a}^l(x\Gamma t_b)\right) \\
 &+ E\left(\mathbf{a}^s\left(x\Gamma t_b + \frac{\pi}{2}\right), \mathbf{a}^s\left(x\Gamma t_b + \frac{\pi}{2}\right)\right), \tag{44}
 \end{aligned}$$

from which the averages  $\hat{E}^{ll\pm}(\varphi)$ ,  $\hat{E}^{sl\pm}(\varphi)$ ,  $\hat{E}^{ss+}(\varphi)$  can be obtained. Note that we did not define  $\hat{E}^{ss-}$ , which would not have physical meaning, as  $-\mathbf{a}^s$  is not on the cone, where all possible  $\mathbf{a}^s$ 's lie. In SM, with  $\Delta\Gamma = 0$ ,  $R(f_b, f_b, t_a, t_b)$  can be obtained as

$$\begin{aligned}
 R(f_a, f_b, t_a, t_b) &= \frac{e^{-\Gamma(t_a+t_b)}}{4} \times \left\{ (|\xi_-|^2 + |\zeta_-|^2) \right. \\
 &\quad - (|\xi_-|^2 - |\zeta_-|^2) \cos(x\Gamma(t_a - t_b)) \\
 &\quad \left. - 2Im(\zeta_-^* \xi_-) \sin(x\Gamma(t_a - t_b)) \right\}, \tag{45}
 \end{aligned}$$

where  $\xi_- \equiv -\left(\frac{p}{q} A_{fa} A_{fb} - \frac{q}{p} \bar{A}_{fa} \bar{A}_{fb}\right)$ ,  $\zeta_- \equiv (A_{fa} \bar{A}_{fb} - \bar{A}_{fa} A_{fb})$ .

In experiments, it is more convenient to use the time-integrated joint decay rate

$$R(f_a, f_b, \Delta t) = \int_0^\infty dt_a R_-(f_a, f_b, t_a, t_a + \Delta t), \tag{46}$$

which is obtained as

$$\begin{aligned}
 R(f_a, f_b, \Delta t) &= \frac{e^{-\Gamma|\Delta t|}}{8\Gamma} \times \left\{ (|\xi_-|^2 + |\zeta_-|^2) \right. \\
 &\quad - (|\xi_-|^2 - |\zeta_-|^2) \cos(x\Gamma\Delta t) \\
 &\quad \left. + 2Im(\zeta_-^* \xi_-) \sin(x\Gamma\Delta t) \right\}, \tag{47}
 \end{aligned}$$

It is more rigorous to test LI of the discrete version of the average correlation functions, rather than that of the continuous version. However, it is experimentally much easier to measure  $N(f_a, f_b, \Delta t) \propto \epsilon_{f_a, f_b} R(f_a, f_b, \Delta t)$  than  $N_{f_a, f_b}(t_a, t_b)$ , consequently it is much easier to test LI in terms of the continuous version of the average correlation functions.

From (45) and (47), it can be seen that in SM,  $R(f_a, f_b, t_b + \Delta t, t_b) = 2\Gamma e^{-\Gamma(t_a+t_b)} e^{\Gamma|\Delta t|} R(f_a, f_b, \Delta t)$ . Consequently,  $\hat{E}(\varphi)$ , as an average of  $E(\phi_a, \phi_b)$  over  $\xi \equiv x\Gamma(t_a + t_b)/2 + \pi/2$ , can be directly related to  $N(f_a, f_b, \Delta t)$  as

$$\begin{aligned}
 \hat{E}^{ll}(\varphi = x\Gamma\Delta t) &= \\
 &\left( \frac{N(l_a^+, l_b^+, \Delta t)}{\epsilon_{l_a^+, l_b^+} |A_{l_a^+}|^2 |A_{l_b^+}|^2} + \frac{N(l_a^-, l_b^-, \Delta t)}{\epsilon_{l_a^-, l_b^-} |\bar{A}_{l_a^-}|^2 |\bar{A}_{l_b^-}|^2} \right)
 \end{aligned}$$

$$\begin{aligned}
 &\left( \frac{N(l_a^+, l_b^-, \Delta t)}{\epsilon_{l_a^+, l_b^-} |A_{l_a^+}|^2 |\bar{A}_{l_b^-}|^2} - \frac{N(l_a^-, l_b^+, \Delta t)}{\epsilon_{l_a^-, l_b^+} |\bar{A}_{l_a^-}|^2 |A_{l_b^+}|^2} \right) \\
 &/ \left( \frac{N(l_a^+, l_b^+, \Delta t)}{\epsilon_{l_a^+, l_b^+} |A_{l_a^+}|^2 |A_{l_b^+}|^2} + \frac{N(l_a^-, l_b^-, \Delta t)}{\epsilon_{l_a^-, l_b^-} |\bar{A}_{l_a^-}|^2 |\bar{A}_{l_b^-}|^2} \right. \\
 &\quad \left. + \frac{N(l_a^+, l_b^-, \Delta t)}{\epsilon_{l_a^+, l_b^-} |A_{l_a^+}|^2 |\bar{A}_{l_b^-}|^2} + \frac{N(l_a^-, l_b^+, \Delta t)}{\epsilon_{l_a^-, l_b^+} |\bar{A}_{l_a^-}|^2 |A_{l_b^+}|^2} \right), \tag{48}
 \end{aligned}$$

$$\begin{aligned}
 \hat{E}^{sl}(\varphi = x\Gamma\Delta t + \frac{\pi}{2}) &= \\
 &\left( \frac{N(S_a^+, l_b^+, \Delta t)}{\epsilon_{S_a^+, l_b^+} |A_{S_a^+}|^2 |A_{l_b^+}|^2} - \frac{N(S_a^-, l_b^-, \Delta t)}{\epsilon_{S_a^-, l_b^-} |A_{S_a^-}|^2 |\bar{A}_{l_b^-}|^2} \right. \\
 &\quad \left. + \frac{N(S_a^+, l_b^-, \Delta t)}{\epsilon_{S_a^+, l_b^-} |A_{S_a^+}|^2 |\bar{A}_{l_b^-}|^2} - \frac{N(S_a^-, l_b^+, \Delta t)}{\epsilon_{S_a^-, l_b^+} |A_{S_a^-}|^2 |A_{l_b^+}|^2} \right) \\
 &/ \left( \frac{N(S_a^+, l_b^+, \Delta t)}{\epsilon_{S_a^+, l_b^+} |A_{S_a^+}|^2 |A_{l_b^+}|^2} + \frac{N(S_a^-, l_b^-, \Delta t)}{\epsilon_{S_a^-, l_b^-} |A_{S_a^-}|^2 |\bar{A}_{l_b^-}|^2} \right. \\
 &\quad \left. + \frac{N(S_a^+, l_b^-, \Delta t)}{\epsilon_{S_a^+, l_b^-} |A_{S_a^+}|^2 |\bar{A}_{l_b^-}|^2} + \frac{N(S_a^-, l_b^+, \Delta t)}{\epsilon_{S_a^-, l_b^+} |A_{S_a^-}|^2 |A_{l_b^+}|^2} \right), \tag{49}
 \end{aligned}$$

$$\begin{aligned}
 \hat{E}^{ss}(\varphi = x\Gamma\Delta t) &= \\
 &\left( \frac{N(S_a^+, S_b^+, \Delta t)}{\epsilon_{S_a^+, S_b^+} |A_{S_a^+}|^2 |A_{S_b^+}|^2} + \frac{N(S_a^-, S_b^-, \Delta t)}{\epsilon_{S_a^-, S_b^-} |A_{S_a^-}|^2 |A_{S_b^-}|^2} \right. \\
 &\quad \left. - \frac{N(S_a^+, S_b^-, \Delta t)}{\epsilon_{S_a^+, S_b^-} |A_{S_a^+}|^2 |A_{S_b^-}|^2} - \frac{N(S_a^-, S_b^+, \Delta t)}{\epsilon_{S_a^-, S_b^+} |A_{S_a^-}|^2 |A_{S_b^+}|^2} \right) \\
 &/ \left( \frac{N(S_a^+, S_b^+, \Delta t)}{\epsilon_{S_a^+, S_b^+} |A_{S_a^+}|^2 |A_{S_b^+}|^2} + \frac{N(S_a^-, S_b^-, \Delta t)}{\epsilon_{S_a^-, S_b^-} |A_{S_a^-}|^2 |A_{S_b^-}|^2} \right. \\
 &\quad \left. + \frac{N(S_a^+, S_b^-, \Delta t)}{\epsilon_{S_a^+, S_b^-} |A_{S_a^+}|^2 |A_{S_b^-}|^2} + \frac{N(S_a^-, S_b^+, \Delta t)}{\epsilon_{S_a^-, S_b^+} |A_{S_a^-}|^2 |A_{S_b^+}|^2} \right). \tag{50}
 \end{aligned}$$

Moreover, the integration over  $\xi$  of  $\hat{E}^\pm(\mathbf{a}, \mathbf{b}) = E(\mathbf{a}, \mathbf{b}) + E(\mathbf{b}, \pm\mathbf{b})$  can be performed independently for the two terms on RHS, consequently,

$$\begin{aligned}
 \hat{E}_{ll}^+(\varphi) &= \hat{E}^{ll}(\varphi) + \hat{E}^{ll}(0), \quad \hat{E}_{ll}^-(\varphi) = \hat{E}^{ll}(\varphi) + \hat{E}^{ll}(\pi) \\
 \hat{E}_{sl}^+(\varphi) &= \hat{E}^{sl}(\varphi) + \hat{E}^{ll}(0), \quad \hat{E}_{sl}^-(\varphi) = \hat{E}^{sl}(\varphi) + \hat{E}^{ll}(\pi) \\
 \hat{E}_{ss}^+(\varphi) &= \hat{E}^{ss}(\varphi) + \hat{E}^{ss}(0). \tag{51}
 \end{aligned}$$

Note that Eqs. (41–43) and (48–50) are mainly for the use in analyzing experimental data. QM result can be obtained simply from  $\langle \mathbf{a}^X, \mathbf{a}^Y | \Psi_- \rangle = -\mathbf{a}^X \cdot \mathbf{a}^Y$ , therefore

$$\begin{aligned}
 \hat{E}^{sl}(\varphi) &= -\sin(2\beta) \cos(\varphi), \quad \hat{E}^{ll}(\varphi) = -\cos(\varphi), \\
 \hat{E}^{ss}(\varphi) &= -\cos^2(2\beta) - \sin^2(2\beta) \cos(\varphi). \tag{52}
 \end{aligned}$$

It is interesting to test our LI using various systems, in which  $\varphi_a$  and  $\varphi_b$  are directly adjusted.



For  $B_d$  mesons, QM result (52) can also be obtained from the definition (36) of correlation functions, with

$$P(X \pm, Y \pm, t_a, t_b) \propto$$

$\left| \langle X \pm, Y \pm | W_a W_b | \Psi(t_a, t_b) \rangle \right|^2$  obtained by substituting LHS of  $R(f_a, f_b, t_a, t_b) \propto \left| \langle f_a, f_b | W_a W_b | \Psi(t_a, t_b) \rangle \right|^2$  with the result (45) of  $R(f_a, f_b, t_a, t_b)$ , and RHS with the joint amplitudes (38–40), and then having  $A_f$  and  $\bar{A}_f$  cancelled. For  $B_d$  mesons, the values of  $\beta$  and  $x$  are given by  $\sin(2\beta) = 0.695$ ,  $x = 0.769$  [97].

The upper bound of a our LI violation can be quantified as

$$g^u(\varphi_1, \varphi_2) \equiv \frac{h_L^u(\varphi_1, \varphi_2) - h_R^u(\varphi_1, \varphi_2)}{|h_L^u(\varphi_1, \varphi_2)|}, \tag{53}$$

where  $h_R^u$  and  $h_L^u(\varphi_1, \varphi_2)$  are RHS and LHS of (32), respectively. The first lower bound can be quantified as

$$g^{d1}(\varphi_1, \varphi_2) = \frac{h_R^{d1}(\varphi_1, \varphi_2) - h_L^{d1}(\varphi_1, \varphi_2)}{|h_L^{d1}(\varphi_1, \varphi_2)|}, \tag{54}$$

where  $h_R^{d1}$  and  $h_L^{d1}$  are RHS and LHS of (33), respectively. The second lower bound can be quantified as

$$g^{d2}(\varphi_1, \varphi_2) = \frac{h_R^{d2}(\varphi_1, \varphi_2) - h_L^{d2}(\varphi_1, \varphi_2)}{|h_L^{d2}(\varphi_1, \varphi_2)|}, \tag{55}$$

where  $h_R^{d2}$  and  $h_L^{d2}$  are RHS and LHS of (34), respectively. Each of these three quantities larger than 0 represents the violation of the corresponding bound of LI.

From  $\partial_{\varphi_1} g^u(\varphi_1, \varphi_2) = \partial_{\varphi_1} g^{d1}(\varphi_1, \varphi_2) = \partial_{\varphi_1} g^{d2}(\varphi_1, \varphi_2) = 0$ , it is determined that the maximum of  $g^u$  is on  $\varphi_1 = \pi$ , while the maxima of  $g^{d1}$  and  $g^{d2}$  are both on  $\varphi_1 = 0$ .  $L_1(\varphi_1 = \pi) = L_2(\varphi_1 = 0) \approx 0.781$ ,  $\theta_1(\varphi_1 = \pi) = \theta_2(\varphi_1 = 0) \approx 0.401$ .

Furthermore, solving  $\partial_{\varphi_2} g^u(\pi, \varphi_2) = 0$  numerically, we find that  $g^u(\pi, \varphi_2)$  reaches its maximum at  $\varphi_2 \approx \pm 2.81$ . We also find numerically that  $g^u(\pi, \varphi_2) > 0$  when  $2.39 < |\varphi_2| < \pi$ . Similarly, solving  $\partial_{\varphi_2} g^{d1}(0, \varphi_2) = 0$  numerically, we find that  $g^{d1}(0, \varphi_2)$  reaches the maximum at  $\varphi_2 \approx \pm 0.336$ . We also find numerically that  $g^{d1}(0, \varphi_2) > 0$  when  $0 < |\varphi_2| < 0.75$ .

Solving  $\partial_{\varphi_2} g^{d2}(0, \varphi_2) = 0$  numerically, we find that  $g^{d2}(0, \varphi_2)$  reaches its maximum at  $\varphi_2 \approx \pm 0.486$ , and we find numerically that  $g^{d2}(0, \varphi_2) > 0$  when  $0 < |\varphi_2| < 1.11$ . The  $\varphi_2$  range of  $g^{d2} > 0$  is larger than that of  $g^{d1} > 0$ . The maxima of  $g^u$ ,  $g^{d1}$  and  $g^{d2}$  are all about 2.7%. The results are depicted in Fig. 2.

A  $B_d$  meson is unstable, and the time interval between the two decays is of the order of the lifetime  $\tau_B$  [71]. So it is better to study the case in which  $\Delta t$  is of the order of  $\tau_B$ , so that the number of events is large. Thus it is easier to test  $g^{d2}$ , because in its violation region,  $\Delta t$  is closer to  $\tau_B$ .

We now focus on how to make measurements to confirm the violation of the second lower bound.  $g^{d2}(\varphi_1, \varphi_2) > 0$  can be found in the regime ( $\varphi_1 = 0, 0 < |\varphi_2| < 1.11$ ), as calculated above. The function  $g^{d2}(\varphi_1, \varphi_2)$  contains  $\hat{E}_{sl}^+(\varphi_1) = \hat{E}^{sl}(\varphi_1) + \hat{E}^{ll}(0)$  and  $\hat{E}_{ss}^+(\varphi_2) = \hat{E}^{ss}(\varphi) + \hat{E}^{ss}(0)$ . Hence one first measures  $\hat{E}^{ll}(\Delta t_1 = 0)$  and  $\hat{E}^{sl}(\varphi_1 = 0) = \hat{E}^{sl}(\Delta t_1 = -\pi/2x\Gamma \approx -2.04\tau_B)$ , as shown in Fig. 3. Thus  $\hat{E}_{sl}^+(\varphi_1 = 0) = \hat{E}^{sl}(\varphi_1 = 0) + \bar{E}^{ll}(\varphi_1 = 0)$  is obtained. One also needs to measure  $\hat{E}^{ss}(\Delta t_2 = 0)$  and  $\hat{E}^{ss}(\Delta t_2)$  with  $0 < |\Delta t_2| < 1.11/x\Gamma \approx 1.44\tau_B$ , such that  $\hat{E}_{ss}^+(\varphi_2)$  with  $0 < |\varphi_2| < 1.11$  is obtained. Thus one obtains  $g^{d2}(\varphi_1, \varphi_2) > 0$  in this regime. The violation is maximal when  $\Delta t_2 \approx 0.486/x\Gamma \approx 0.633\tau_B$ , then  $g^{d2}(\varphi_1, \varphi_2) \approx 2.7\%$ , as shown in Fig. 3. Typically, the resolution of the signal is proportional to the inverse of square of event numbers [71]. Therefore it can be estimated that the expected signal of LI violation can be observed when the event number is about  $10^4$ – $10^5$ , which can be achieved in current experiments [64].

It is also possible to test LI in polarization-entangled baryon-antibaryon pairs produced in, say,  $J/\Psi \rightarrow \Lambda \bar{\Lambda}$  decays, where the polarizations of  $\Lambda$  and  $\bar{\Lambda}$  can be measured through the angular distribution of the momenta of their decay products pions. However, the effective measuring directions satisfying the Malus' law are yet to be found out.

If using other systems such as photon polarizations to test our LI,  $\theta_s$  may become a variable. The results of  $\partial_{\varphi_1} g^u(\varphi_1, \varphi_2) = \partial_{\varphi_1} g^{d1}(\varphi_1, \varphi_2) = \partial_{\varphi_1} g^{d2}(\varphi_1, \varphi_2) = 0$  do not depend on  $\theta_s$ , hence their maxima are still at  $\varphi_1 = \pi, 0, 0$ , respectively.  $g^u(\theta_s, \pi, \varphi_2)$ ,  $g^{d1}(\theta_s, 0, \varphi_2)$  and  $g^{d2}(\theta_s, 0, \varphi_2)$  as functions of  $\theta_s$  and  $\varphi_2$  are shown in Fig. 4. Interestingly, in a certain range of  $\varphi_2$ , for any value of  $\theta_s$ , except 0 and  $\pi/2$ , we always have  $g^{d2} > 0$ , that is, the second lower bound is always violated.

Furthermore, we numerically found the maximal violations of the three bounds are all 3.87482% when  $\theta_s = 1.18208$ , i.e.

$$\begin{aligned} g^u(1.18208, \pm\pi, \pm 2.7373) &= g^{d1}(1.18208, 0, \pm 0.404296) \\ &= g^{d2}(1.18208, 0, \pm 0.437399) \\ &= 3.87482\%. \end{aligned} \tag{56}$$

It is also found that

$$g^{d1}(1.18208, 0, \varphi_2) > 0, \text{ when } 0 < |\varphi_2| < 1.0734, \tag{57}$$

$$g^{d2}(1.18208, 0, \varphi_2) > 0, \text{ when } 0 < |\varphi_2| < 1.17078. \tag{58}$$

The latter is wider, as shown in Fig 5.

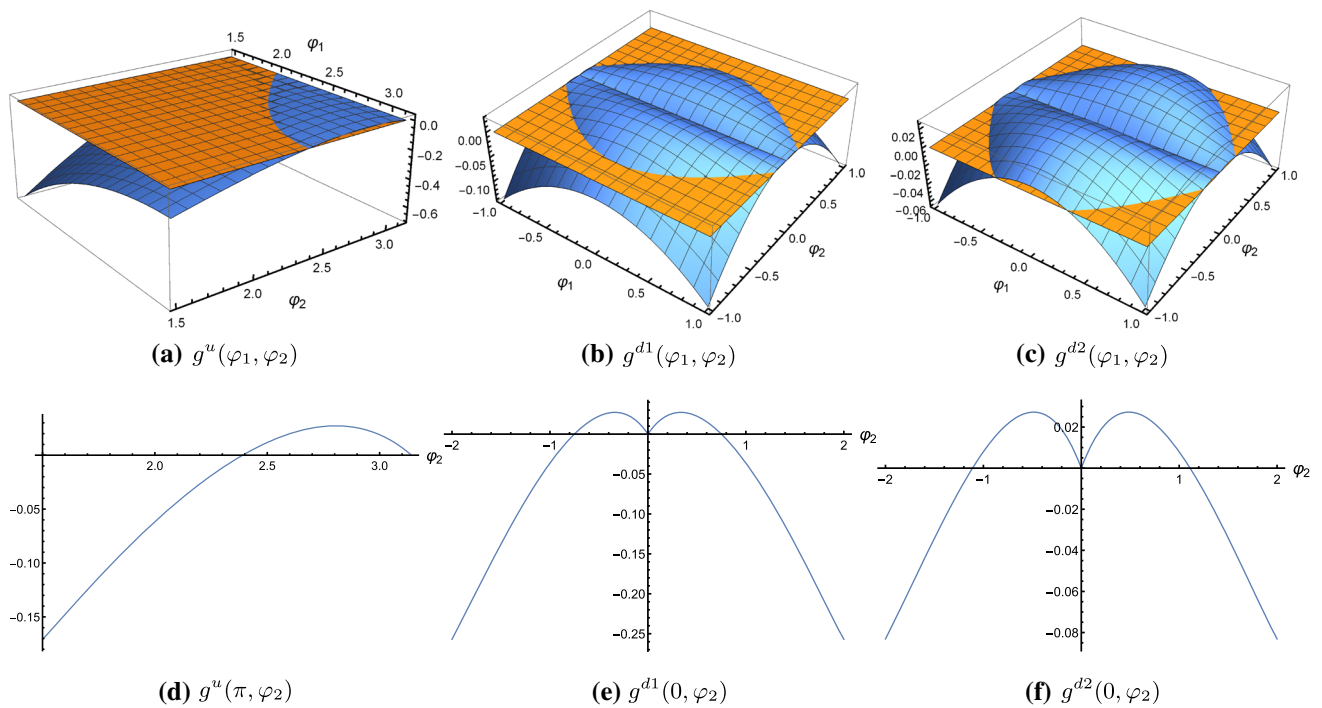


**Fig. 2** LI violation of entangled  $B_d$  mesons.  $\theta_s$  is fixed to be  $\sin^{-1} 0.695$ . Our LI is violated when  $g^u(\varphi_1, \varphi_2) > 0$  or  $g^{d1}(\varphi_1, \varphi_2) > 0$  or  $g^{d2}(\varphi_1, \varphi_2) > 0$ .  $g^u > 0$  when  $\varphi_1 = \pi, 2.39 < |\varphi_2| < \pi$ , and the maximum is at  $\varphi_1 = \pm\pi, \varphi_2 \approx \pm 2.81$ .  $g^{d1} > 0$  when  $\varphi_1 = 0, 0 < |\varphi_2| < 0.75$ , and the maximum is at  $\varphi_1 = 0, \varphi_2 \approx \pm 0.336$ .  $g^{d2} > 0$  when  $\varphi_1 = 0, 0 < |\varphi_2| < 1.11$ , and the maximum is at  $\varphi_1 = 0, \varphi_2 \approx \pm 0.486$ . The maxima are all about 2.7%

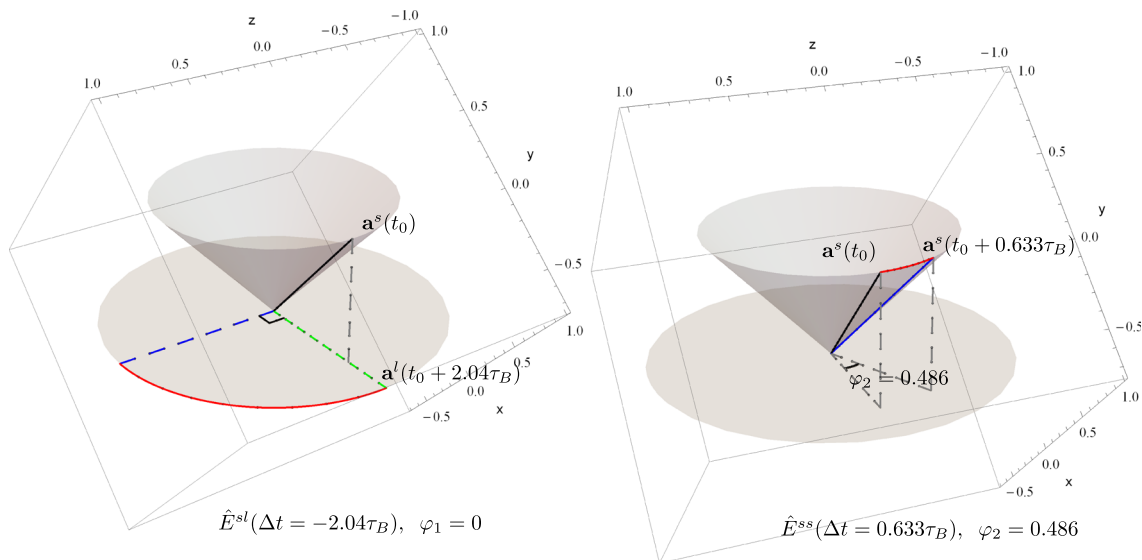


**Fig. 3** The correlation functions to be measured. The left picture represents  $\hat{E}^{sl}(\Delta t = \pi/2x\Gamma \approx 2.04\tau_B) = \hat{E}^{sl}(\varphi_1 = 0)$ . The right picture represents  $\hat{E}^{ss}(\Delta t = 0.486/x\Gamma \approx 0.633\tau_B) = \hat{E}^{ss}(\varphi_2 \approx 0.486)$ . They give rise to  $g^{d1}(\varphi_1 = 0, \varphi_2 \approx 0.486)$ , which maximally violates the second lower bound of our LI

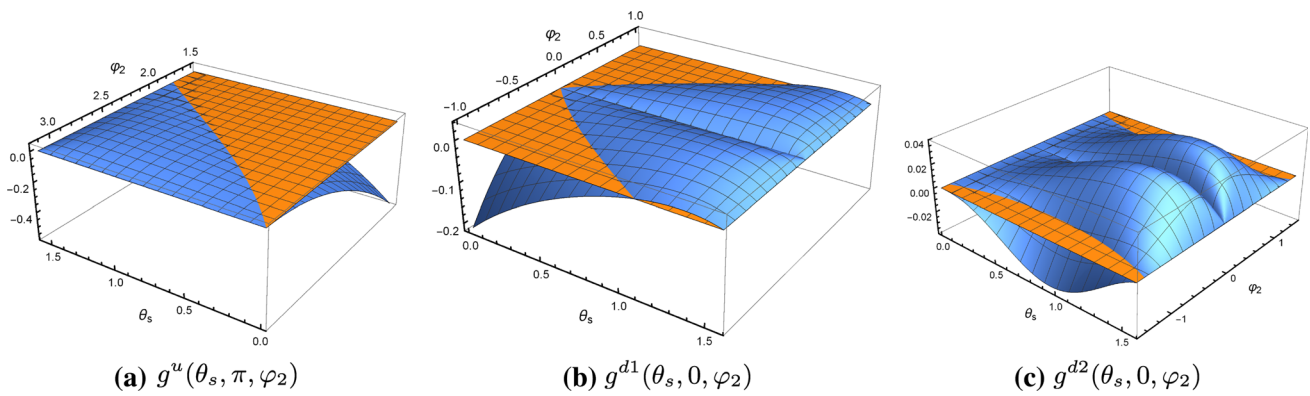


**Fig. 4** LI violation in case  $\theta_s$  is a variable. The maxima of  $g^u$ ,  $g^{d1}$  and  $g^{d2}$  are still at  $\varphi_1 = \pi, 0, 0$ , respectively.  $g^u(\theta_s, \pi, \varphi_2)$ ,  $g^{d1}(\theta_s, 0, \varphi_2)$  and  $g^{d2}(\theta_s, 0, \varphi_2)$  are functions of  $\theta_s$  and  $\varphi_2$

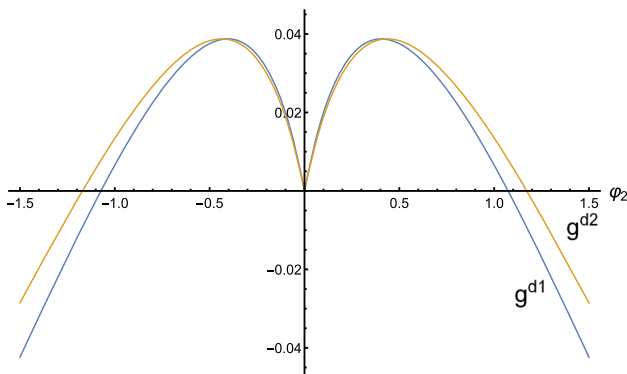


**Fig. 5** The two lower bounds are maximally violated on  $\theta_s = 1.18208$ ,  $\varphi_1 = 0$ . Shown here are the dependence of  $g^{d1}(\theta_s = 1.18208, \varphi_1 = 0, \varphi_2)$  and  $g^{d2}(\theta_s = 1.18208, \varphi_1 = 0, \varphi_2)$  on  $\varphi_2$ .  $g^{d1} > 0$  when  $0 < |\varphi_2| < 1.0734$ , while  $g^{d2} > 0$  when  $0 < |\varphi_2| < 1.17078$

### 6 Summary and discussions

To summarize, we have extended the CNHV theories to include the case that the measuring settings, together with the measurement outcomes, are not externally fixed, but determined by HVs. The outcomes of those measurements with the same settings give averages satisfying Malus' Law and make up correlation functions. We show that such is the case of meson decays, which could be determined by HVs at the source of the meson pairs. This extension does not change the validity of LI. Therefore, entangled meson pairs can be used to test LI.

We find that for a  $B_d$  meson, the effective measuring directions appearing in Malus' Law are on a cone and a plane, corresponding to semileptonic decays and decays to CP eigenstates, respectively. For such effective measuring directions, we present a new LI. This can be tested in  $C = -1$  entangled state of  $B^0 - \bar{B}^0$  pairs, within the present experimental capability. The expected violation is estimated quantitatively, using the indirect CP violation and other parameters. Our LI

is violated if there is indirect CP violation. There may be profound reason for this surprising connection. Besides, our new LI can also be tested in other systems such as photon polarizations, where the measuring directions are simply directions externally fixed.

**Acknowledgements** This work is supported by National Science Foundation of China (Grant Nos. 11574054 and 11947066).

**Data Availability Statement** This manuscript has no associated data or the data will not be deposited. [Authors' comment: It is purely theoretical.]

**Open Access** This article is licensed under a Creative Commons Attribution 4.0 International License, which permits use, sharing, adaptation, distribution and reproduction in any medium or format, as long as you give appropriate credit to the original author(s) and the source, provide a link to the Creative Commons licence, and indicate if changes were made. The images or other third party material in this article are included in the article's Creative Commons licence, unless indicated otherwise in a credit line to the material. If material is not included in the article's Creative Commons licence and your intended use is not permitted by statutory regulation or exceeds the permitted use, you will need to obtain permission directly from the copyright holder. To view a copy of this licence, visit <http://creativecommons.org/licenses/by/4.0/>.  
Funded by SCOAP<sup>3</sup>.

### A Two inequalities

We derive a new LI, for  $\mathbf{a}^l(\phi_l)$  on a plane and  $\mathbf{a}^s(\theta_s, \phi_s)$  on a cone.

For each particle, each measurement yields an outcome  $A = A(\mathbf{u}, \mathbf{v}, \tilde{\mathbf{a}}(\lambda), \tilde{\mathbf{b}}(\lambda), \lambda) = \pm 1$  or  $B = B(\mathbf{v}, \mathbf{u}, \tilde{\mathbf{b}}(\lambda), \tilde{\mathbf{a}}(\lambda), \lambda) = \pm 1$ . Using  $-1 + \int d\lambda \rho'_{\mathbf{u},\mathbf{v},\mathbf{a},\mathbf{b}}(\lambda) |A + B| = \int d\lambda \rho'_{\mathbf{u},\mathbf{v},\mathbf{a},\mathbf{b}}(\lambda) AB = 1 - \int d\lambda \rho'_{\mathbf{u},\mathbf{v},\mathbf{a},\mathbf{b}}(\lambda) |A - B|$ , where  $\rho'_{\mathbf{u},\mathbf{v},\mathbf{a},\mathbf{b}}(\lambda) \equiv \rho_{\mathbf{u},\mathbf{v},\mathbf{v}}(\lambda) \delta(\tilde{\mathbf{a}}(\lambda) - \mathbf{a}) \delta(\tilde{\mathbf{b}}(\lambda) - \mathbf{b})$ , and  $\bar{A} = \int d\lambda \rho'_{\mathbf{u},\mathbf{v},\mathbf{a},\mathbf{b}}(\lambda) A(\mathbf{u}, \mathbf{v}, \tilde{\mathbf{a}}(\lambda), \tilde{\mathbf{b}}(\lambda), \lambda) = \mathbf{u} \cdot \mathbf{a}$ ,  $\bar{B} = \int d\lambda \rho'_{\mathbf{u},\mathbf{v},\mathbf{a},\mathbf{b}}(\lambda) B(\mathbf{v}, \mathbf{u}, \tilde{\mathbf{b}}(\lambda), \tilde{\mathbf{a}}(\lambda), \lambda) = \mathbf{v} \cdot \mathbf{b}$ , one finds  $1 - \int d\mathbf{u} d\mathbf{v} F(\mathbf{u}, \mathbf{v}) |\mathbf{u} \cdot \mathbf{a} - \mathbf{v} \cdot \mathbf{b}|$

$\mathbf{a} - \mathbf{v} \cdot \mathbf{b} \geq E(\mathbf{a}, \mathbf{b}) \geq -1 + \int d\mathbf{u}d\mathbf{v}F(\mathbf{u}, \mathbf{v})|\mathbf{u} \cdot \mathbf{a} + \mathbf{v} \cdot \mathbf{b}|$  [15, 16].

Furthermore [23], considering  $|\mathbf{u} \cdot \mathbf{a} + \mathbf{v} \cdot \mathbf{b}| + |\mathbf{u} \cdot \mathbf{b} + \mathbf{v} \cdot \mathbf{b}| \geq |\mathbf{u} \cdot \mathbf{a} + \mathbf{v} \cdot \mathbf{b} - (\mathbf{u} \cdot \mathbf{b} + \mathbf{v} \cdot \mathbf{b})| = |\mathbf{u} \cdot (\mathbf{a} - \mathbf{b})|$ , and  $|\mathbf{u} \cdot \mathbf{a} - \mathbf{v} \cdot \mathbf{b}| + |\mathbf{u} \cdot \mathbf{b} + \mathbf{v} \cdot \mathbf{b}| \geq |\mathbf{u} \cdot (\mathbf{a} + \mathbf{b})|$ , one obtains

$$\hat{E}^+(\mathbf{a}, \mathbf{b}) \geq -2 + \int d\mathbf{u}F(\mathbf{u})|\mathbf{u} \cdot (\mathbf{a} - \mathbf{b})|, \tag{59a}$$

$$\hat{E}^-(\mathbf{a}, \mathbf{b}) \leq 2 - \int d\mathbf{u}F(\mathbf{u})|\mathbf{u} \cdot (\mathbf{a} + \mathbf{b})|. \tag{59b}$$

with  $\hat{E}^+(\mathbf{a}, \mathbf{b}) \equiv E(\mathbf{a}, \mathbf{b}) + E(\mathbf{b}, \mathbf{b})$  and  $\hat{E}^-(\mathbf{a}, \mathbf{b}) \equiv E(\mathbf{a}, \mathbf{b}) + E(\mathbf{b}, -\mathbf{b})$ .

All the results remain valid in the special case that  $\tilde{\mathbf{a}}(\lambda)$  and  $\tilde{\mathbf{b}}(\lambda)$  are externally set to be always  $\mathbf{a}$  and  $\mathbf{b}$  respectively.

### B Upper bound

Suppose  $\mathbf{a} = \mathbf{a}^s(\theta_s, \phi_a)$ ,  $\mathbf{b} = \mathbf{a}^l(\phi_b)$ . Then Eqs. (59b) reads

$$\begin{aligned} \hat{E}^-(\mathbf{a}^s(\theta_s, \phi_a), \mathbf{a}^l(\phi_b)) &\leq 2 - \int_0^\pi \sin \theta_u d\theta_u \\ &\times \int_0^{2\pi} d\phi_u F(\theta_u, \phi_u) \\ &\left| \mathbf{u}(\theta_u, \phi_u) \cdot (\mathbf{a}^s(\phi_a) + \mathbf{a}^l(\phi_b)) \right|. \end{aligned} \tag{60}$$

As shown in Fig. 6,

$$\begin{aligned} \mathbf{a}^s(\theta_s, \phi_a) + \mathbf{a}^l(\phi_b) &= L_1(\theta_s, \varphi) (\sin(\theta_1) \cos(\xi + \alpha_1), \\ &\sin(\theta_1) \sin(\xi_1), \cos(\theta_1)), \end{aligned} \tag{61}$$

where

$$\begin{aligned} L_1(\theta_s, \varphi) &\equiv |\mathbf{a}^s + \mathbf{a}^l| = \sqrt{2 + 2 \cos(\varphi) \sin(\theta_s)}, \\ \theta_1(\theta_s, \varphi) &= \cos^{-1} \frac{\cos(\theta_s)}{\sqrt{2 + 2 \cos(\varphi) \sin(\theta_s)}}, \end{aligned}$$

$\varphi = \phi_a - \phi_b$ ,  $\xi = \frac{\phi_a + \phi_b}{2}$ ,  $\alpha_1$  is an angle depending on  $\varphi$  and  $\theta_s$  while independent of  $\xi$ , as shown in Fig. 6. With  $0 < \theta_s < \pi/2$ , we have  $\sin(\theta_1) > 0$ ,  $\cos(\theta_1) > 0$ .

Rewriting  $\hat{E}^-(\mathbf{a}^s(\theta_s, \phi_a), \mathbf{a}^l(\phi_b))$  as  $\hat{E}_{sl}^-(\theta_s, \xi, \varphi)$ , then

$$\begin{aligned} \hat{E}_{sl}^-(\theta_s, \varphi) &\equiv \int \frac{d\xi}{2\pi} \hat{E}_{sl}^-(\theta_s, \xi, \varphi) \\ &\leq 2 - L_1(\theta_s, \varphi) \int_0^{2\pi} \frac{d\xi}{2\pi} \int_0^\pi \sin \theta_u d\theta_u \int_0^{2\pi} d\phi_u F(\theta_u, \phi_u) \\ &\times |\sin(\theta_u) \sin(\theta_1) \cos(\phi_u - \xi - \alpha_1) + \cos(\theta_u) \cos(\theta_1)| \\ &\leq 2 - L_1(\theta_s, \varphi) \int_0^\pi \sin \theta_u d\theta_u F(\theta_u) \cos(\theta_1) |\cos(\theta_u)|, \end{aligned} \tag{62}$$

where  $F(\theta_u) \equiv \int_0^{2\pi} d\phi_u F(\theta_u, \phi_u)$ . In obtaining the second inequality, we have used

$$\begin{aligned} &\int_0^{2\pi} \frac{d\xi}{2\pi} |\sin(\theta_1) \cos(\phi_u - \xi - \alpha_1) \sin(\theta_u) \\ &+ \cos(\theta_1) \cos(\theta_u)| \\ &= \int_0^{2\pi} \frac{d\xi}{2\pi} |\sin(\theta_1) \cos(\xi) \sin(\theta_u) + \cos(\theta_1) \cos(\theta_u)| \\ &\geq \cos(\theta_1) |\cos(\theta_u)|, \end{aligned} \tag{63}$$

as

$$\begin{aligned} \int_0^{2\pi} d\xi |\cos(\xi + \beta) + a| &= \int_0^{2\pi} d\xi |\cos(\xi) + a| \\ &= 4\text{Re} \left( \sqrt{1 - a^2} + a \sin^{-1}(a) \right) \\ &\geq 2\pi |a|, \end{aligned}$$

where  $a$  and  $\beta$  are arbitrary real numbers.

The case that the two vectors are on a same plane is a special case of above with  $\theta_s = \pi/2$ . In this special case,  $L_1 = 2 \cos(\varphi/2)$ ,  $\theta_1 = \pi/2$ . Hence

$$\begin{aligned} \hat{E}_{ll}^-(\theta_s, \varphi) &\equiv \int \frac{d\xi}{2\pi} E \left( \mathbf{a}^l \left( \xi + \frac{\varphi}{2} \right), \mathbf{a}^l \left( \xi - \frac{\varphi}{2} \right) \right) \\ &\leq 2 - 2 \cos \left( \frac{\varphi}{2} \right) \int_0^{2\pi} \frac{d\xi}{2\pi} \int_0^\pi \sin \theta_u d\theta_u F(\theta_u) \\ &|\cos(\xi) \sin(\theta_u)| \\ &= 2 - \frac{4}{\pi} \cos \left( \frac{\varphi}{2} \right) \int_0^\pi \sin \theta_u d\theta_u F(\theta_u) |\sin(\theta_u)|, \end{aligned} \tag{64}$$

where  $\int_0^{2\pi} d\xi |\cos(\xi)| = 4$  is used.

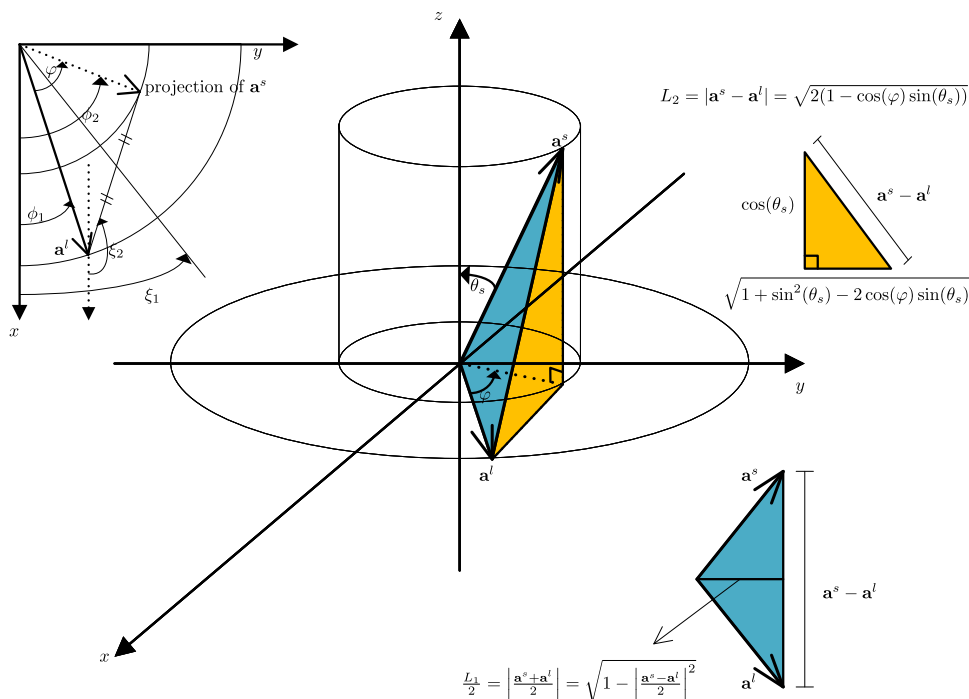
Therefore one obtains

$$\begin{aligned} \hat{E}_{sl}^-(\theta_s, \varphi_1) &+ \frac{\pi \cos(\theta_1(\theta_s, \varphi_1)) L_1(\theta_s, \varphi_1)}{4 \cos(\frac{\varphi_2}{2})} \hat{E}_{ll}^-(\theta_s, \varphi_2) \\ &\leq 2 \left( 1 + \frac{\pi \cos(\theta_1(\theta_s, \varphi_1)) L_1(\theta_s, \varphi_1)}{4 \cos(\frac{\varphi_2}{2})} \right) \\ &- \cos(\theta_1(\theta_s, \varphi_1)) L_1(\theta_s, \varphi_1) \\ &\times \int_0^\pi \sin \theta_u d\theta_u F(\theta_u) (|\cos(\theta_u)| + |\sin(\theta_u)|). \end{aligned} \tag{65}$$

Using  $\int_0^\pi d\theta_u \sin(\theta_u) F(\theta_u) = 1$  and  $|\cos(\theta_u)| + |\sin(\theta_u)| \geq 1$ , one obtains

$$\begin{aligned} \hat{E}_{sl}^-(\theta_s, \varphi_1) &+ \frac{\pi \cos(\theta_1(\theta_s, \varphi_1)) L_1(\theta_s, \varphi_1)}{4 \cos(\frac{\varphi_2}{2})} \hat{E}_{ll}^-(\theta_s, \varphi_2) \\ &\leq 2 \left( 1 + \frac{\pi \cos(\theta_1(\theta_s, \varphi_1)) L_1(\theta_s, \varphi_1)}{4 \cos(\frac{\varphi_2}{2})} \right) \end{aligned}$$

**Fig. 6** Geometric relations among  $\mathbf{a}^s, \mathbf{a}^l, \mathbf{a}^s + \mathbf{a}^l$  and  $\mathbf{a}^s - \mathbf{a}^l$



$$- \cos(\theta_1(\theta_s, \varphi_1)) L_1(\theta_s, \varphi_1). \tag{66}$$

**C Lower bounds**

From Eq. (59a), one obtains

$$\hat{E}^+(\mathbf{a}^s(\theta_s, \phi_a), \mathbf{a}^l(\phi_b)) \geq -2 + \int_0^\pi \sin \theta_u d\theta_u \int_0^{2\pi} d\phi_u \times F(\theta_u, \phi_u) \left| \mathbf{u}(\theta_u, \phi_u) \cdot (\mathbf{a}^s(\theta_s, \phi_a) - \mathbf{a}^l(\phi_b)) \right|. \tag{67}$$

As shown in Fig. 6,

$$\mathbf{a}^s(\theta_s, \phi_a) - \mathbf{a}^l(\phi_b) = L_2(\theta_s, \varphi) (\sin(\theta_2) \cos(\xi + \alpha_2), \sin(\theta_2) \sin(\xi_2), \cos(\theta_2)), \tag{68}$$

where

$$L_2(\theta_s, \varphi) \equiv |\mathbf{a}^s - \mathbf{a}^l| = \sqrt{2 - 2 \cos(\varphi) \sin(\theta_s)}$$

$$\theta_2 = \cos^{-1} \frac{\cos(\theta_s)}{\sqrt{2 - 2 \cos(\varphi) \sin(\theta_s)}},$$

$\alpha_2$  is an angle depending on  $\theta_s$  and  $\varphi$  while independent of  $\xi$ .

Rewriting  $\hat{E}^+(\mathbf{a}^s(\theta_s, \phi_a), \mathbf{a}^l(\phi_b))$  as  $\hat{E}_{sl}^+(\theta_s, \xi, \varphi)$ ,

$$\hat{E}_{sl}^+(\theta_s, \varphi) \equiv \int \frac{d\xi}{2\pi} \hat{E}_{sl}^+(\theta_s, \xi, \varphi)$$

$$\geq -2 + L_2(\theta_s, \varphi) \int_0^{2\pi} \frac{d\xi}{2\pi} \int_0^\pi \sin \theta_u d\theta_u$$

$$\times \int_0^{2\pi} d\phi_u F(\theta_u, \phi_u)$$

$$\times |\sin(\theta_u) \sin(\theta_2) \cos(\phi_u - \xi - \alpha_2) + \cos(\theta_u) \cos(\theta_2)|. \tag{69}$$

Considering the special case of  $\theta_s = \pi/2$ , one obtains

$$\hat{E}_{ll}^+(\varphi) \geq -2 + 2 \left| \sin\left(\frac{\varphi}{2}\right) \right| \int_0^{2\pi} \frac{d\xi}{2\pi} \int_0^\pi \sin \theta_u d\theta_u \times F(\theta_u) |\cos(\xi) \sin(\theta_u)|. \tag{70}$$

Therefore

$$\hat{E}_{sl}^+(\theta_s, \varphi_1) + \frac{\pi \cos(\theta_2(\theta_s, \varphi_1)) L_2(\theta_s, \varphi_1)}{4 \left| \sin\left(\frac{\varphi_2}{2}\right) \right|} \hat{E}_{ll}^+(\theta_s, \varphi_2)$$

$$\geq -2 \left( 1 + \frac{\pi \cos(\theta_2(\theta_s, \varphi_1)) L_2(\theta_s, \varphi_1)}{4 \left| \sin\left(\frac{\varphi_2}{2}\right) \right|} \right)$$

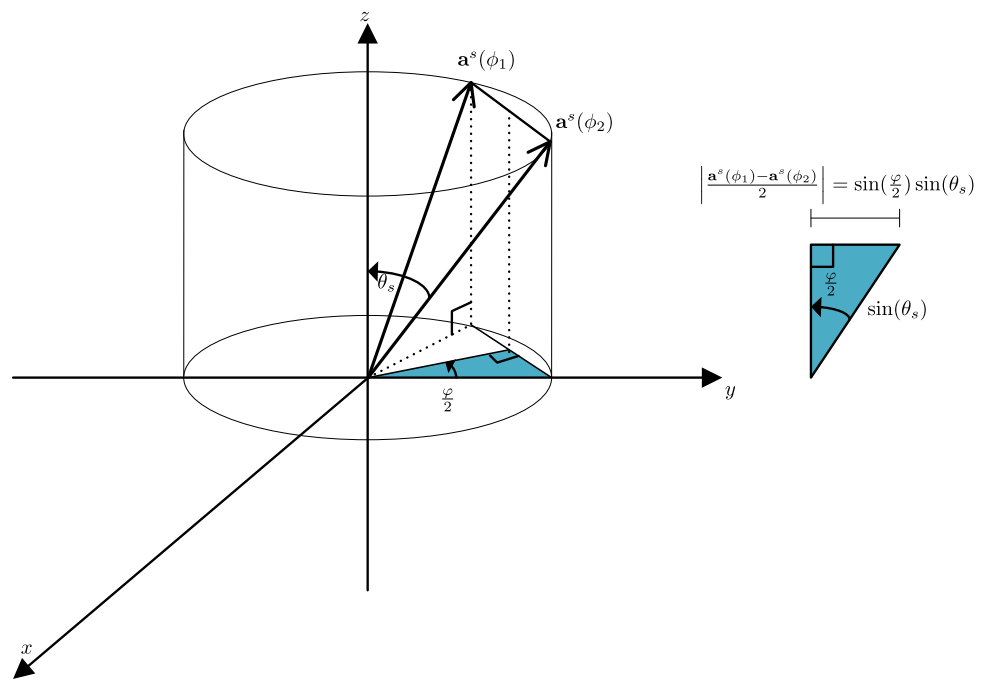
$$+ \cos(\theta_2(\theta_s, \varphi_1)) L_2(\theta_s, \varphi_1). \tag{71}$$

We find the second lower bound, in terms of correlation function  $\hat{E}^{ss+}(\theta_s, \phi_a, \phi_b)$  between  $\mathbf{a}^s(\theta_s, \phi_a)$  and  $\mathbf{a}^s(\theta_s, \phi_b)$ , which are on a same plane, with  $|\mathbf{a}^s(\theta_s, \phi_a) - \mathbf{a}^s(\theta_s, \phi_b)| = 2 \sin(\theta_s) \sin(\varphi/2)$ , as shown in Fig. 7. We find

$$\hat{E}_{ss}^+(\theta_s, \varphi) \geq -2 + 2 \sin(\theta_s) \left| \sin\left(\frac{\varphi}{2}\right) \right|$$

$$\times \int_0^{2\pi} \frac{d\xi}{2\pi} \int_0^\pi \sin \theta_u d\theta_u F(\theta_u) |\cos(\xi) \sin(\theta_u)|. \tag{72}$$

**Fig. 7** Geometric relations of  $\mathbf{a}^s(\phi_a)$ ,  $\mathbf{a}^s(\phi_b)$  and  $\mathbf{a}^s(\phi_a) - \mathbf{a}^s(\phi_b)$



Therefore,

$$\begin{aligned} & \hat{E}_{sl}^+(\theta_s, \varphi_1) + \frac{\pi \cos(\theta_2(\theta_s, \varphi_1)) L_2(\theta_s, \varphi_1)}{4 \sin(\theta_s) \left| \sin\left(\frac{\varphi_2}{2}\right) \right|} \hat{E}_{ss}^+(\varphi_2) \\ & \geq -2 \left( 1 + \frac{\pi \cos(\theta_2(\theta_s, \varphi_1)) L_2(\theta_s, \varphi_1)}{4 \sin(\theta_s) \left| \sin\left(\frac{\varphi_2}{2}\right) \right|} \right) \\ & \quad + \cos(\theta_2) L_2(\theta_s, \varphi_1). \end{aligned} \tag{73}$$

Equations (66), (71) and (73) comprise our LI.

**D LI in terms of discrete versions of average correlation functions**

In the discrete version, Eq. (64) is changed to

$$\begin{aligned} \hat{E}_{sl}^-(\theta_s, \varphi) & \equiv \frac{1}{N} \sum_{n=1}^N \hat{E}_{sl}^-\left(\theta_s, \frac{2n\pi}{N}, \varphi\right) \\ & \leq 2 - L_1(\theta_s, \varphi) \int_0^\pi \sin \theta_u d\theta_u \int_0^{2\pi} d\phi_u F(\theta_u, \phi_u) \\ & \quad \times \frac{1}{N} \sum_{n=1}^N \left| \sin(\theta_u) \sin(\theta_1(\theta_s, \varphi)) \cos(\phi_u - \alpha_1 - \frac{2n\pi}{N}) \right. \\ & \quad \left. + \cos(\theta_u) \cos(\theta_1(\theta_s, \varphi)) \right|. \end{aligned} \tag{74}$$

Noting

$$\frac{1}{N} \sum_{n=1}^N \left| \cos\left(\frac{2n\pi}{N} + \beta\right) + a \right| \geq |a| \tag{75}$$

for arbitrary real numbers  $\beta$  and  $a$ , we can change Eq. (63) to

$$\begin{aligned} & \frac{1}{N} \sum_{n=1}^N \left| \sin(\theta_1(\theta_s, \varphi)) \cos\left(\phi_u - \frac{2n\pi}{N} - \alpha_1\right) \sin(\theta_u) \right. \\ & \quad \left. + \cos(\theta_1) \cos(\theta_u) \right| \geq \cos(\theta_1(\theta_s, \varphi)) |\cos(\theta_u)|. \end{aligned} \tag{76}$$

which is then used in Eq. (74). One finds

$$\hat{E}_{sl}^-(\theta_s, \varphi) \leq 2 - L_1(\theta_s, \varphi) \int_0^\pi \sin \theta_u d\theta_u F(\theta_u) \cos(\theta_1) |\cos(\theta_u)|. \tag{77}$$

Similarly, one has

$$\begin{aligned} \hat{E}_{sl}^+(\theta_s, \varphi) & \geq -2 + L_2(\theta_s, \varphi) \int_0^\pi \sin \theta_u d\theta_u F(\theta_u) \\ & \quad \cos(\theta_{n_2}) |\cos(\theta_u)|. \end{aligned} \tag{78}$$

On the other hand, Eq. (64) can be changed to

$$\begin{aligned} \hat{E}_{ll}^-(\varphi') & \equiv \frac{1}{N} \sum_{n=1}^N E\left(\mathbf{a}^l\left(\frac{2n\pi}{N} + \frac{\varphi'}{2}\right), \mathbf{a}^l\left(\frac{2n\pi}{N} - \frac{\varphi'}{2}\right)\right) \\ & \leq 2 - 2 \cos\left(\frac{\varphi'}{2}\right) \frac{1}{N} \sum_{n=1}^N \int_0^\pi \sin \theta_u d\theta_u \end{aligned}$$

$$\times F(\theta_u) \left| \cos\left(\frac{2n\pi}{N}\right) \sin(\theta_u) \right|. \tag{79}$$

Using  $\frac{1}{N} \sum_{n=1}^N |\cos(\frac{2n\pi}{N} + \beta)| \geq \frac{1}{N} \cot(\frac{\pi}{2N}) \equiv u_N$  [18], one obtains

$$\hat{E}_{II}^-(\varphi) \leq 2 - 2u_N \cos\left(\frac{\varphi}{2}\right) \int_0^\pi \sin\theta_u d\theta_u F(\theta_u) |\sin(\theta_u)|. \tag{80}$$

Similarly, we have

$$\begin{aligned} \hat{E}_{II}^+(\varphi) &\leq -2 + 2u_N \cos\left(\frac{\varphi}{2}\right) \int_0^\pi \sin\theta_u d\theta_u F(\theta_u) |\sin(\theta_u)|. \\ \hat{E}_{ss}^+(\varphi) &\geq -2 + 2u_N \sin(\theta_s) \left| \sin\left(\frac{\varphi}{2}\right) \right| \\ &\quad \times \int_0^\pi \sin\theta_u d\theta_u F(\theta_u) |\sin(\theta_u)|. \end{aligned} \tag{81}$$

With Eqs. (77), (78), (80) and (81), we establish LI in terms of the discrete version of average correlation functions,

$$\begin{aligned} \hat{E}_{sl}^-(\varphi_1) + \frac{\cos(\theta_1)L_1(\theta_s, \varphi_1)}{2u_N \cos(\frac{\varphi_2}{2})} \hat{E}_{II}^-(\varphi_2) \\ \leq 2 \left( 1 + \frac{\cos(\theta_1)L_1(\theta_s, \varphi_1)}{2u_N \cos(\frac{\varphi_2}{2})} \right) - \cos(\theta_1)L_1(\theta_s, \varphi_1), \\ \hat{E}_{sl}^+(\varphi_1) + \frac{\cos(\theta_2)L_2(\theta_s, \varphi_1)}{2u_N |\sin(\frac{\varphi_2}{2})|} \hat{E}_{II}^+(\varphi_2) \\ \geq -2 \left( 1 + \frac{\cos(\theta_2)L_2(\theta_s, \varphi_1)}{2u_N |\sin(\frac{\varphi_2}{2})|} \right) + \cos(\theta_2)L_2(\theta_s, \varphi_1). \\ \hat{E}_{sl}^+(\varphi_1) + \frac{\cos(\theta_2)L_2(\theta_s, \varphi_1)}{2u_N \sin(\theta_s) |\sin(\frac{\varphi_2}{2})|} \hat{E}_{ssN}^+(\varphi_2) \\ \geq -2 \left( 1 + \frac{\cos(\theta_2)L_2(\theta_s, \varphi_1)}{2u_N \sin(\theta_s) |\sin(\frac{\varphi_2}{2})|} \right) + \cos(\theta_2)L_2(\theta_s, \varphi_1). \end{aligned} \tag{82}$$

**References**

1. A. Einstein, B. Podolsky, N. Rosen, Can quantum–mechanical description of physical reality be considered complete? *Phys. Rev.* **47**, 777–780 (1935)
2. E. Schrödinger, Die Gegenwärtige Situation in der Quantenmechanik. *Naturwissenschaften* **23**, 807 (1935)
3. J.S. Bell, On the einstein podolsky rosen paradox. *Physics* **1**, 195–200 (1964)
4. J.F. Clauser et al., Proposed experiment to test local hidden-variable theories. *Phys. Rev. Lett.* **23**, 880 (1969)
5. A. Aspect, P. Grangier, G. Roger, Experimental test of Bell’s inequalities using time-varying analyzers. *Phys. Rev. Lett.* **49**, 1804 (1982)
6. G. Weihs, T. Jennewein, C. Simon, H. Weinfurter, A. Zeilinger, Violation of Bell’s inequality under strict einstein locality conditions. *Phys. Rev. Lett.* **81**, 5039 (1998)

7. M. Giustina et al., Bell violation using entangled photons without the fair-sampling assumption. *Nature* **497**, 227 (2013)
8. B.G. Christensen et al., Detection–Loophole-free test of quantum nonlocality, and applications. *Phys. Rev. Lett.* **111**, 130406 (2013)
9. B. Hensen et al., Loophole-Free Bell inequality violation using electron spins separated by 1.3 kilometres, *Nature* **526**, 682 (2015)
10. M. Giustina et al., Significant–Loophole-free test of Bell’s theorem with entangled photons. *Phys. Rev. Lett.* **115**, 250401 (2015)
11. L.K. Shalm et al., Strong Loophole-free test of local realism. *Phys. Rev. Lett.* **115**, 250402 (2015)
12. J. Handsteiner et al., Cosmic bell test: measurement settings from milky way stars. *Phys. Rev. Lett.* **118**, 060401 (2017)
13. M. Li et al., Test of local realism into the past without detection and locality loopholes. *Phys. Rev. Lett.* **121**, 080404 (2018)
14. The BIG Bell Test Collaboration, Challenging Local realism with human choices. *Nature* **557**, 212 (2018)
15. A.J. Leggett, Nonlocal hidden-variable theories and quantum mechanics: an incompatibility theorem. *Found. Phys.* **33**, 1469 (2003)
16. S. Gröblacher, T. Paterek, R. Kaltenbaek, V.C. Brukner, M. Zukowski, M. Aspelmeyer, A. Zeilinger, An Experimental test of non-local realism, *Nature* **446**, 871 (2007)
17. T. Paterek, A. Fedrizzi, S. Gröblacher, T. Jennewein, M. Zukowski, M. Aspelmeyer, A. Zeilinger, Experimental test of nonlocal realistic theories without the rotational symmetry assumption. *Phys. Rev. Lett.* **99**, 210406 (2007)
18. C. Branciard et al., Experimental Falsification of leggett’s nonlocal variable model. *Phys. Rev. Lett.* **99**, 210407 (2007)
19. M. D. Eisaman et al. Experimental test of nonlocal realism using a fiber-based source of polarization-entangled photon pairs., *Phys. Rev. A* **77**, 032339 (2008)
20. J. Romero et al., Violation of leggett inequalities in orbital angular momentum subspaces. *New J. Phys.* **12**(12), 123007 (2010)
21. Y. Hasegawa et al., Falsification of Leggett’s model using neutron matter waves. *New J. Phys.* **14**(2), 023039 (2012)
22. F. Cardano et al., Violation of Leggett-type inequalities in the spin–orbit degrees of freedom of a single photon. *Phys. Rev. A* **88**, 032101 (2013)
23. Stephen Parrott, Comments on An Experimental Test of Non-Local Realism by S. Groeblacher, T. Paterek, R. Kaltenbaek, C. Brukner, M. Zukowski, M. Aspelmeyer, and A. Zeilinger, *Nature* **446**, 871 (2007), [arXiv:0707.3296](https://arxiv.org/abs/0707.3296)
24. R. Colbeck, R. Renner, Hidden variable models for quantum theory cannot have any local part. *Phys. Rev. Lett.* **101**, 050403 (2008)
25. C. Branciard et al., Testing Quantum correlations versus single-particle properties within Leggett’s model and beyond. *Nat. Phys.* **4**, 681 (2008). [arXiv:0801.2241](https://arxiv.org/abs/0801.2241)
26. H. Su, J. Chen, C. Wu, D. Deng, C.H. Oh, Testing Leggett’s inequality using Aharonov–Casher effect. *Sci. Rep.* **3**, 2492 (2013)
27. T. D. Lee and C. N. Yang, reported by Lee at Argonne National Lab on May 28, 1960 (unpublished)
28. D.R. Inglis, Completeness of quantum mechanics and Charge–conjugation correlations of theta particles. *Rev. Mod. Phys* **33**, 1 (1961)
29. T.B. Day, Demonstration of quantum mechanics in the large. *Phys. Rev.* **121**, 1204 (1961)
30. H. J. Lipkin, CP Violation and coherent decays of kaon pairs , *ibid* **176**, 1715 (1968)
31. See, e.g., J. Six, Test of the non separability of the  $K^0 \bar{K}^0$  System, *Phys. Lett. B* **114**, 200 (1982)
32. F. Selleri, Einstein locality and the  $K^0 \bar{K}^0$  system. *Lett. Nuovo Cimento* **36**, 521 (1983)
33. A. Datta, D. Home, Quantum non-separability versus local realism: a new test using the  $B^0 \bar{B}^0$  system. *Phys. Lett. A* **119**, 3 (1986)

34. A. Afriat, F. Selleri, *The einstein, podolsky and rosen paradox in atomic, nuclear and particle physics* (Plenum Press, New York, 1998)
35. R.A. Bertlmann, W. Grimus, How devious are deviations from quantum mechanics: the case of the  $B^0\bar{B}^0$  system. *Phys. Rev. D* **58**, 034014 (1998)
36. R.A. Bertlmann, W. Grimus, B.C. Hiesmayr, Quantum mechanics, Furry's hypothesis, and a measure of decoherence in the  $K^0\bar{K}^0$  system. *Phys. Rev. D* **60**, 114032 (1999)
37. R.A. Bertlmann, W. Grimus, Model for decoherence of entangled beauty. *Phys. Rev. D* **64**, 056004 (2001)
38. A. Apostolakis et al., (CLEAR collaboration), An EPR experiment testing the nonseparability of the  $K^0 - \bar{K}^0$  wave function. *Phys. Lett. B* **422**, 339 (1998)
39. A. Di Domenico (KLOE Collaboration), CPT symmetry and quantum mechanics tests in the neutral kaon system at KLOE, *Found. Phys.* **40**, 852 (2010)
40. F. Ambrosino et al., (KLOE Collaboration), First observation of quantum interference in the process  $\phi \rightarrow K(S)K(L) \rightarrow \pi^+\pi^-\pi^+\pi^-$ : a test of quantum mechanics and cpt symmetry. *Phys. Lett. B* **642**, 315 (2006)
41. G. Amelino-Camelia et al., Physics with the KLOE-2 experiment at the upgraded DAΦNE. *Eur. Phys. J. C* **68**, 619 (2010)
42. A. Go (Belle Collaboration), Observation of Bell inequality violation in b mesons, *J. Mod. Opt.* **51**, 991 (2004), [arXiv:quant-ph/0310192](https://arxiv.org/abs/quant-ph/0310192)
43. A. Go et al., (Belle Collaboration), Measurement of Einstein–Podolsky–Rosen-type flavor entanglement in  $\Upsilon(4S) \rightarrow B^0\bar{B}^0$  decays. *Phys. Rev. Lett.* **99**, 131802 (2007)
44. A.J. Bevan et al., The Physics of the B Factories. *Eur. Phys. J. C* **74**, 3026 (2014)
45. R.M. Baltrusaitis et al., (MARK-III Collaboration), Direct measurements of charmed  $D$  meson hadronic branching fractions. *Phys. Rev. Lett.* **56**, 2140 (1986)
46. J. Adler et al., (MARK-III Collaboration), A reanalysis of charmed  $D$  meson branching fractions. *Phys. Rev. Lett.* **60**, 89 (1988)
47. B. Aubert et al., (BABAR Collaboration), Measurement of time-dependent CP asymmetry in  $B^0 \rightarrow c\bar{c}K^{(*)0}$  decays. *Phys. Rev. D* **79**, 072009 (2009). [arXiv:0902.1708](https://arxiv.org/abs/0902.1708)
48. M. Ablikim et al., (BESIII Collaboration), Measurement of the  $D \rightarrow K^-\pi^+$  strong phase difference in  $\psi(3770) \rightarrow D^0\bar{D}^0$ . *Phys. Lett. B* **734**, 227 (2014). [arXiv:1404.4691](https://arxiv.org/abs/1404.4691)
49. M. Ablikim et al. (BESIII Collaboration), Measurement of  $y_{CP}$  in  $D^0 - \bar{D}^0$  oscillation using quantum correlations in  $e^+e^- \rightarrow D^0\bar{D}^0$  at  $\sqrt{s}=3.773\text{GeV}$ . *Phys. Lett. B* **744**, 339 (2015), [arXiv:1501.01378](https://arxiv.org/abs/1501.01378)
50. M. Gronau, Y. Grossman, J.L. Rosner, Measuring  $D^0 - \bar{D}^0$  mixing and relative strong phases at a charm factory. *Phys. Lett. B* **508**, 37 (2001). [arXiv:hep-ph/0103110](https://arxiv.org/abs/hep-ph/0103110)
51. A.F. Falk, A.A. Petrov, Measuring gamma cleanly with CP-tagged B(s) and B(d) decays. *Phys. Rev. Lett.* **85**, 252 (2000)
52. D. Atwood, A.A. Petrov, Lifetime differences in heavy mesons with time independent measurements. *Phys. Rev. D* **71**, 054032 (2005). [arXiv:hep-ph/0207165](https://arxiv.org/abs/hep-ph/0207165)
53. D. Atwood, A. Soni, Measuring  $B_s$  width difference at the  $\Upsilon(5s)$  using quantum entanglement. *Phys. Rev. D* **82**, 036003 (2010)
54. M.C. Bañuls, J. Bernabéu, CP, T and CPT Versus temporal asymmetries for entangled states of the  $B_d$ -system. *Phys. Lett.* **464**, 117 (1999). [arXiv:hep-ph/9908353](https://arxiv.org/abs/hep-ph/9908353)
55. M.C. Bañuls, J. Bernabéu, Studying Indirect violation of CP, T and CPT in a B-factory. *Nucl. Phys. B* **590**, 19 (2000). [arXiv:hep-ph/0005323](https://arxiv.org/abs/hep-ph/0005323)
56. J. Bernabéu, F. J. Botella, M. Nebot, Novel T-Violation observable open to any pair of decay channels at meson factories, [arXiv:1309.0439](https://arxiv.org/abs/1309.0439)
57. J. Bernabéu, F. J. Botella, M. Nebot, Genuine T, CP, CPT asymmetry parameters for the entangled  $B_d$  system, *JHEP*, **06**, 100 (2016), [arXiv:1605.03925](https://arxiv.org/abs/1605.03925)
58. Y. Shi, Exact Theorems Concerning CP and CPT Violations in  $C = -1$  Entangled State of Pseudoscalar Neutral Mesons, *Eur. Phys. J. C* **72**, 1907 (2012) Z. J. Huang and Y. Shi, Extracting rephase-invariant CP and CPT violating parameters from asymmetries of time-ordered integrated rates of correlated decays of entangled mesons, *Eur. Phys. J. C* **72**, 1900 (2013)
59. Y. Shi, Some exact results on CP and CPT violations in a  $C = -1$  entangled pseudoscalar neutral meson pair. *Eur. Phys. J. C* **73**, 2506 (2013). [arXiv:1306.2676](https://arxiv.org/abs/1306.2676)
60. Z.J. Huang, Y. Shi,  $CP$  and  $CPT$  violating parameters determined from the joint decays of  $C = +1$  entangled neutral pseudoscalar mesons. *Phys. Rev. D* **89**, 016018 (2014). [arXiv:1307.4459](https://arxiv.org/abs/1307.4459)
61. H.J. Lipkin, Simple symmetries in EPR-correlated decays of kaon and b-meson pairs with  $CP$  violation. *Phys. Lett. B* **219**, 474–480 (1989)
62. I. Dunietz, J. Hauser, J.L. Rosner, Proposed experiment addressing  $CP$  and  $CPT$  violation in the  $K^0 - \bar{K}^0$  system. *Phys. Rev. D* **35**, 2166 (1987)
63. C.D. Buchanan et al., Testing  $CP$  and  $CPT$  violation in the neutral kaon system at a  $\phi$  factory. *Phys. Rev. D* **45**, 4088 (1992)
64. B. Aubert et al., (BABAR Collaboration), Improved measurement of  $CP$  violation in neutral  $B$  decays to  $c\bar{c}s$ . *Phys. Rev. Lett.* **99**, 171803 (2007). [arXiv:hep-ex/0703021](https://arxiv.org/abs/hep-ex/0703021)
65. Z.Z. Xing,  $D^0 - \bar{D}^0$  mixing and  $CP$  violation in neutral  $D$ -meson decays. *Phys. Rev. D* **55**, 196 (1997). [arXiv:hep-ph/9606422](https://arxiv.org/abs/hep-ph/9606422)
66. H.B. Li, M.Z. Yang,  $D^0 - \bar{D}^0$  mixing in  $\Upsilon(1S) \rightarrow D^0\bar{D}^0$  decay at super-B. *Phys. Rev. D* **74**, 094016 (2006). [arXiv:hep-ph/0610073](https://arxiv.org/abs/hep-ph/0610073)
67. J.P. Lees et al., (BaBar Collaboration), Observation of Time Reversal Violation in the  $B^0$  Meson System. *Phys. Rev. Lett.* **109**, 211801 (2012). [arXiv:1207.5832](https://arxiv.org/abs/1207.5832)
68. J. Bernabéu, F. Martinez-Vidal, P. Villanueva-Perez, Time reversal violation from the entangled  $B^0\bar{B}^0$  system. *JHEP* **1208**, 064 (2012). [arXiv:1203.0171](https://arxiv.org/abs/1203.0171)
69. J. Bernabéu, F. Martinez-Vidal, Colloquium: time-reversal violation with quantum-entangled B mesons, *Rev. Mod. Phys.* **87**, 165 (2015), [arXiv:1410.1742](https://arxiv.org/abs/1410.1742). J. Bernabéu, A. Di Domenico, and P. Villanueva-Perez, Direct test of time-reversal symmetry in the entangled neutral kaon system at a  $\phi$ -factory, *Nucl. Phys. B* **868**, 102 (2013), [arXiv:1208.0773](https://arxiv.org/abs/1208.0773)
70. E.M. Henley, Time reversal symmetry. *Int. J. Mod. Phys. E* **22**, 1330010 (2013)
71. Yu Shi and Ji-Chong Yang, Time reversal symmetry violation in entangled pseudoscalar neutral charmed mesons, *Phys. Rev. D* **98**, 075019 (2018), [arXiv:1612.07628](https://arxiv.org/abs/1612.07628)
72. J. Bernabéu, N.E. Mavromatos, J. Papavassiliou, Novel type of  $CPT$  violation for correlated EPR states. *Phys. Rev. Lett.* **92**, 131601 (2004). [arXiv:hep-ph/0310180](https://arxiv.org/abs/hep-ph/0310180)
73. E. Álvarez, J. Bernabéu,  $\Delta t$ -dependent equal-sign dilepton asymmetry and CPTV effects in the symmetry of the  $B^0 - \bar{B}^0$  entangled state. *JHEP* **0611**, 087 (2006). [arXiv:hep-ph/0605211](https://arxiv.org/abs/hep-ph/0605211)
74. Y. Shi, High energy quantum teleportation using neutral kaons. *Phys. Lett. B* **641**, 75 (2006)
75. Y. Shi, Erratum to: “High energy quantum teleportation using neutral kaons”. *Phys. Lett. B*, **641**, 492 (2006)
76. Y. Shi, Y.L. Wu, CP measurement in quantum teleportation of neutral mesons. *Eur. Phys. J. C* **55**, 477 (2008)
77. BESIII, Polarization and entanglement in baryon-antibaryon pair production in electron–positron annihilation, *Nat. Phys.* **15**, 631–638 (2019), [arXiv:1808.08917](https://arxiv.org/abs/1808.08917)
78. See, e.g., P. H. Eberhard, Testing the non-locality of quantum theory in two-kaon systems, *Nucl. Phys. B* **398**, 155 (1993)
79. A. Di Domenico, Testing quantum mechanics in the neutral kaon system at a phi factory, *ibid* **450**, 293 (1995) [arXiv:hep-ex/0312032](https://arxiv.org/abs/hep-ex/0312032)



80. F. Uchiyama, Generalized Bell inequality in two neutral kaon systems. *Phys. Lett. A* **231**, 295 (1997)
81. F. Benatti, R. Floreanini, Bell's locality and  $\epsilon'/\epsilon$ . *Phys. Rev. D* **57**, R1332 (1998)
82. A. Bramon, M. Nowakowski, Bell inequalities for entangled pairs of neutral kaons. *Phys. Rev. Lett.* **83**, 1 (1999)
83. R.A. Bertlmann, W. Grimus, B.C. Hiesmayr, Bell inequality and CP violation in the neutral kaon system. *Phys. Lett. A* **289**, 21 (2001). [arXiv:quant-ph/0107022](https://arxiv.org/abs/quant-ph/0107022)
84. M. Genovese, C. Novero, E. Predazzi, Can experimental tests of Bell inequalities performed with pseudoscalar mesons be definitive? *Phys. Lett. B* **513**, 401 (2001). [arXiv:hep-ph/0103298](https://arxiv.org/abs/hep-ph/0103298)
85. N. Gisin, A. Go, EPR test with photons and kaons: analogies. *Am. J. Phys.* **69**, 264 (2001)
86. R.H. Dalitz, G. Garbarino, Local realistic theories and quantum mechanics for the two-neutral-kaon system. *Nucl. Phys. B* **606**, 483 (2001). [arXiv:quant-ph/0011108](https://arxiv.org/abs/quant-ph/0011108)
87. N.A. Tönqvist, Suggestion for Einstein–Podolsky–Rosen experiments using reactions like  $e^+e^- \rightarrow \Lambda\bar{\Lambda} \rightarrow \pi^-p\pi^+\bar{p}$ . *Found. Phys.* **11**, 171 (1981)
88. P. Privitera, Decay correlations in  $e^+e^- \rightarrow \tau^+\tau^-$  as a test of quantum mechanics. *Phys. Lett. B* **275**, 172 (1992)
89. S.A. Abel, M. Dittmar, H. Dreiner, Testing locality at colliders via Bell's inequality? *Phys. Lett. B* **280**, 304 (1992)
90. J. Li, C.F. Qiao, Feasibility of Testing local hidden variable theories in a charm factory. *Phys. Rev. D* **74**, 076003 (2006)
91. X. Hao et al., Testing Bell Inequality at experiments of high energy physics. *Chin. Phys. C* **34**, 311 (2010). [arXiv:0904.1000](https://arxiv.org/abs/0904.1000)
92. B.C. Hiesmayr, Limits Of quantum information in weak interaction processes of hyperons. *Sci. Rep.* **5**, 11591 (2015)
93. M. Laméhi-Rachti, W. Mittig, Quantum mechanics and hidden variables: a test of Bell's inequality by the measurement of the spin correlation in low-energy proton–proton scattering. *Phys. Rev. D* **14**, 2543 (1976)
94. R.A. Bertlmann, A. Bramon, G. Garbarino, B.C. Hiesmayr, Violation of a Bell inequality in particle physics experimentally verified? *Phys. Lett. A* **332**, 355 (2004). [arXiv:quant-ph/0409051](https://arxiv.org/abs/quant-ph/0409051)
95. A. Bramon, R. Escribano, G. Garbarino, Bell's inequality tests: from photons to B-mesons. *J. Mod. Opt.* **52**, 1681 (2005). [arXiv:quant-ph/0410122](https://arxiv.org/abs/quant-ph/0410122)
96. A. Bramon, R. Escribano, G. Garbarino, Bell's inequality tests with meson-antimeson pairs. *Found. Phys.* **36**, 563 (2006). [quant-ph/0501069](https://arxiv.org/abs/quant-ph/0501069)
97. M. Tanabashi et al., (Particle data group), review of particle physics. *Phys. Rev. D* **98**, 030001 (2018)